Integrating multispectral imagery, airborne lidar and field inventory data for invasive species management in southern coastal areas of USA.

by

Nisham Thapa

A thesis submitted to the Graduate Faculty of
Auburn University
in partial fulfillment of the
requirements for the Degree of
Master of Science in Forestry

Auburn, Alabama
Dec 10, 2022

Keywords: Invasive species, Remote sensing,
Lidar, Classifier, Distribution, Spread

Approved by

Dr. Lana L. Narine, Chair, Assistant Professor, College of Forestry, Wildlife and Environment, Auburn University
Dr. Zhaofei (Joseph) Fan, Associate Professor, College of Forestry, Wildlife and Environment, Auburn University
Dr. Nancy J. Loewenstein, Extension Specialist, College of Forestry, Wildlife and Environment, Auburn University

Abstract

Invasive plant species have imposed severe threats to native ecosystems, worldwide. Among the well-established species, Chinese tallow (Triadica sebifera) and Chinese privet (Ligustrum sinense) are among the worst invasive plant species of the southern United States. Therefore, it is crucial to understand their distribution and spread mechanism for management implications. The objectives of this work were to: (1) develop a spatially explicit distribution map of invasive Triadica sebifera and Ligustrum sinense using NAIP imagery and airborne lidar in coastal Alabama, USA, and (2) assess the pattern and factors supporting spread of Chinese tallow in coastal plant community. For the first objective, free and publicly available remote sensing data i.e., National Agriculture Imagery Program (NAIP) imagery and airborne light detection and ranging (lidar) data, were used to compare three image classification methods, representing unsupervised, supervised and machine learning techniques, respectively: (1) Iterative Self-Organizing Data Analysis Technique (ISODATA) clustering, (2) Maximum Likelihood, and (3) Random Forest (RF). The maximum overall accuracy of 98.62% was obtained using the RF model with lidar-derived products and NAIP imagery.

For the second objective, two sampling approaches, simple random sampling and line transect sampling were used to conduct a field inventory in May 2021. Data analysis was carried out using statistical approaches such as correlation analysis and Zero Inflated Negative Binomial (ZINB) regression analysis. The results of the study showed that the community structure influences distribution of Chinese tallow. Additionally, factors such as soil moisture, elevation, proximity to roads, forest type, use of overstory trees by birds, and overland water flow events dispersing seeds have a major impact on the prevalence of Chinese tallow invasion.

The outcomes from this study include an initial baseline inventory of critical invasive species in the region that supports larger-scale mapping and the factors that contribute to the spread of Chinese tallow. These findings are expected to aid in Chinese tallow management decisions in future and facilitate development of a framework for monitoring invasives.

Acknowledgments

I would like to express my sincere gratitude to the academic supervisor, Dr. Lana L. Narine for her incessant guidance, motivation, and support. She has always been the source of encouragement and inspiration throughout the academic journey. I would like to extend my heartful appreciation to Dr. Zhaofei (Joseph) Fan and Dr. Nancy J. Loewenstein for their supervision during course work and contribution as a committee member of the project. After that, I would like to thank Alabama Agricultural Experiment Station and Hatch program of the National Institute of Food and Agriculture, United States Department of Agriculture for funding the project. And I would like to thank Dr. Shaoyang Yang for his contribution in field data collection and valuable insights for data analysis. I would also like to acknowledge Kasip Tiwari, Schyler Brown, Eian Davis, and Cam Boland from Geospatial Analytics Lab of Auburn University for their support and suggestions. I would additionally like to thank Kasip Tiwari for helping me with field data collection.

Finally, I would like to especially thank my parents Pawan Thapa, Manju Thapa, and brother Prajwol Thapa for their never-ending love and support throughout my educational endeavor.

Table of Contents

List of Tables

List of Figures

Chapter 1: Introduction

Southern forests of the United States (US) are valuable economically and ecologically. They are most productive for timber and wood products, support plant biodiversity, seasonal migratory birds, and a variety of wildlife habitat (Guntenspergen & Vairin, 1998; Sui, 2015). Historically, forest types such as loblolly-shortleaf pine, longleaf-slash pine, oak-gum-cypress, oak-hickory, and oak-pine dominated the southern US (Zimmerman et al., 2001). However, less than 5% of the original area of the longleaf-slash pine ecosystem remains today (Van Lear et al., 2005) due to several factors, such as biological invasion, land conversion and urbanization. Moreover, native ecosystems and plant species listed as endangered have been critically threatened by invasive plant species (Wilcove et al., 1998). Due to their capacity to interfere with ecological functions and the related costs of their spread, they are a global problem.

Numerous studies have shown that invasive plant species have potential to lower biodiversity, alter habitat structure, change nutrient cycling, and modify fire regimes (Fan et al., 2021; Randall, 2015; Simberloff et al., 2013; Zedler & Kercher, 2004). Invasive species are causing 42% decline in endangered and threatened species in the US (Order, 1999). In addition, the removal of invasive plant species established in forested areas of the southern US is incredibly expensive. For instance, the annual cost of invasion climbed from $2 billion in 1960-1969 to $ 21 billion in 2010- 2020 (Fantle-Lepczyk et al., 2022).

Biological invasion into a native ecosystem depends on space, time, community structure and ecosystem functions. It can be classified into five stages: transport, introduction, establishment, spread and impact (Blackburn et al., 2011). Invasive species are introduced accidentally through transportation, and travel, or intentionally for food, fuel, lumber, oil, and aesthetic purposes. Once introduced, they pass through captivity/cultivation stages and only become established after they pass through survival and growth-related biotic resistance processes. The spread stage takes place at the regional and landscape scale, and is driven by propagule pressure, species traits, landscape patterns, climate conditions and disturbance regimes (Lockwood et al., 2013).

Southern forests are affected by multiple disturbances that promote the growth of invasive plant species. Hurricanes are the most severe disturbance in the coastal region, bringing storm water, flooding, and land-use change. Wildfire occurrence often increases after severe

hurricanes because of debris accumulation (Myers & Van Lear, 1998). In addition, there are anthropogenic disturbances such as prescribed fire, timber extraction, fire lines, and construction of roads (Fan et al., 2018). These disturbances can promote invasive species seed dispersal and seedling establishment in southern coastal forests (Fan et al., 2012; Hood & Naiman, 2000; Pile et al., 2017; Yang, 2019). Studies have found that supporting factors such as propagule pressure, seed dispersal modes, canopy closure, tree density, ground cover, habitat edge types, ecosystem type, distance to seed sources facilitate the spread of invasive species (Fan et al., 2018; Yang, 2019; Yang et al., 2021).

Several invasive plant species are well established in forests of the US. Among those, *Triadica sebifera* (Chinese tallow) and *Ligustrum sinense* (Chinese privet) are problematic in the coastal region of southeastern US and are spreading inland rapidly (ALIPC, 2019; Miller et al., 2013). Both invasive plant species are native of China and were introduced in the US for ornamental purposes. Chinese tallow was also introduced to make wax and oil from the fruit in the eighteenth century (Howes, 1949). Chinese tallow is commonly known as popcorn tree, tallow tree, Florida aspen, or chicken tree (Jubinsky & Anderson, 1996). It is a fast-growing, deciduous tree, producing up to 310,000 seeds per year (Gray, 1950) and can start to bear seed at three years of age (Godfrey, 1988). It is highly adaptable to areas dominated by flooding (Pattison & Mack, 2009; Rogers & Siemann, 2003; Yang, 2019). Chinese tallow threatens the productivity of native forest resources as well as its composition, structure, and sustainability (Webster et al., 2006).

Chinese privet is an ornamental shrub that grows rapidly and can reach up to 9 m (Greene & Blossey, 2014). It adversely affects wetland ecosystem processes including leaf litter breakdown, nutrient cycling and carbon storage (Hudson et al., 2014). Additionally, it has negative relationship with native plant communities, especially native herbaceous species (Cash et al., 2020). Due high seed production (Yang, 2019), broad environmental tolerance (Pattison & Mack, 2009), dominance in floodplain areas (Foard, 2014), colonization by root sprouts, and seed dispersal modes such as water and birds (Fan et al., 2018; Yang, 2019), Chinese tallow and Chinese privet are establishing successfully and spreading prominently in coastal areas.

It is difficult and expensive to control Chinese tallow and Chinese privet after they are well established in an ecosystem. The average control cost of Chinese tallow is estimated to be $100 thousand per ha (Wang, 2011) and the control cost of privet is estimated to range from

$216–$1820 per ha (Benez-Secanho et al., 2018). Due to the several uncertainties, such as interaction at population, community and ecosystem level, associated with the control of Chinese tallow and Chinese privet, the most effective and low cost management option is early detection and rapid removal of them (Lockwood et al., 2013). Understanding distribution and spread of Chinese tallow and Chinese privet in a coastal region will help identify and evaluate how associated factors initially support the spread of Chinese tallow. This information will further help land managers to make management decisions related to rapid removal and controlling spread of Chinese tallow invasion from freshly invaded coastal region.

Remote sensing is a potentially useful tool for mapping and monitoring invasive plant species. Multi-temporal and multispectral capabilities of remote sensing techniques make it possible to monitor native and invasive species over time (Nagendra et al., 2013). Several studies (Asner, 2008; Bork & Su, 2007; Hantson et al., 2012; Hawthorne et al., 2015; Kim et al., 2020; Liang et al., 2020) have found integration of high-resolution multispectral imagery and active remote sensing techniques such as lidar, quite beneficial for increased accuracy of invasive species mapping. Lidar uses laser light to obtain three-dimensional information (Popescu, 2007). It has been used to accurately estimate forest structural characteristics such as canopy heights, stand volume, basal area, and above-ground biomass (Dubayah & Drake, 2000). Asner et al. (2008) demonstrated the benefit of lidar to detect woody invasive tree species when combined with aerial imagery. Hantson et al. (2012) showed that utilizing lidar-derived products with Maximum Likelihood classification improved overall classification accuracy for woody invasive species from 39% to 50%. Bork and Su (2007) found that the integration of lidar and imagery helped in distinguishing shrub vegetation from tall trees as compared to aerial imagery alone.

Research regarding remote sensing detection of Chinese tallow and Chinese privet is limited, especially over large areas. However, several studies have demonstrated the use of freely available remote sensing data to map the distribution of Chinese tallow (Ill et al., 2002; Joshi et al., 2004; Nagendra et al., 2013; Niphadkar & Nagendra, 2016; Ramsey & Rangoonwala, 2018; Randall, 2015). Cash et al. (2020) and Hawthorne et al. (2015) used remote sensing data for mapping Chinese privet.

The overall goal was to investigate the integrated use of lidar, multispectral imagery and field data inventory for invasive species management in the southern coastal region of United States. The primary objectives of the study were to:

Objective 1: Develop a spatially explicit distribution map of invasive *Triadica sebifera* and *Ligustrum sinense* using NAIP imagery and airborne lidar in coastal Alabama, USA. For this objective, different approaches for mapping Chinese tallow and Chinese privet in coastal region of Alabama, using multispectral imagery and airborne lidar data and derived products were investigated.

Objective 2: Assess the pattern and factors supporting spread of Chinese tallow in coastal plant community: A study conducted in Mississippi Sandhill Crane National Wildlife Refuge, Mississippi, USA. For this objective, field data inventory was carried out, and data analysis was done using statistical approaches such as correlation analysis and ZINB regression analysis.

The two main objectives mentioned above are presented in the thesis as two independent but related studies in Chapter 2 and 3, respectively. Chapter 2 studies the integrated use of lidar and multispectral imagery for mapping the distribution of Chinese tallow and Chinese privet in the southern coastal region of Alabama, US. Chapter 3 studies the pattern and spread of Chinese tallow in coastal region of US. Overall conclusions for both studies, are presented in Chapter 4.

References

ALIPC. (2019). Alabama's 10 worst Invasive Weeds. https://www.se-eppc.org/alabama/

Asner, G. P., Knapp, D.E., Kennedy-Bowdoin, Ty., Jones, M.O., Martin, R. E., Boardman, J., and Hughes, R. F. (2008). Invasive species detection in Hawaiian rainforests using airborne imaging spectroscopy and Lidar. *Remote Sensing of Environment, 112*(5), 1942-1955.

Benez-Secanho, F. J., Grebner, D. L., Ezell, A. W., & Grala, R. K. (2018). Financial trade-offs associated with controlling Chinese privet (*Ligustrum sinense* Lour.) in forestlands in the southern USA. *Journal of Forestry, 116*(3), 236-244.

Blackburn, T. M., Pyšek, P., Bacher, S., Carlton, J. T., Duncan, R. P., Jarošík, V., . . . Richardson, D. M. (2011). A proposed unified framework for biological invasions. *Trends in ecology evolution and Development, 26*(7), 333-339.

Bork, E. W., & Su, J. G. (2007). Integrating LIDAR data and multispectral imagery for enhanced classification of rangeland vegetation: A meta analysis. *Remote Sensing of Environment, 111*(1), 11-24.

Cash, J. S., Anderson, C. J., & Marzen, L. (2020). Evaluating free and simple remote sensing methods for mapping Chinese privet (*Ligustrum sinense*) invasions in hardwood forests. *SN Applied Sciences, 2*(5), 1-11.

Dubayah, R. O., & Drake, J. B. (2000). Lidar remote sensing for forestry. *Journal of forestry, 98*(6), 44-46.

Fan, Z., Yang, S., Cheng, N., Liu, X., Song, A., & Dong, L. (2021). Invasibility of fire-managed ecosystems to the Chinese tallow tree (*Triadica sebifera*) in the lower Gulf Coastal Plain, USA: Mechanisms and key factors at the landscape level. *Forest Ecology and Management 479*, 118539.

Fan, Z., Yang, S., & Liu, X. (2018). Spatiotemporal patterns and mechanisms of Chinese tallowtree (*Triadica sebifera*) spread along edge habitat in a coastal landscape, Mississippi, USA. *Invasive Plant Science Management, 11*(3), 117-126.

Fan, Z., Yuan, T., & Michael K, C. (2012). Factors associated with the spread of Chinese tallow in East Texas forestlands. *Open Journal of Ecology, 2012*.

Fantle-Lepczyk, J. E., Haubrock, P. J., Kramer, A. M., Cuthbert, R. N., Turbelin, A. J., Crystal-Ornelas, R., . . . Courchamp, F. (2022). Economic costs of biological invasions in the United States. *Science of the Total Environment, 806*, 151318.

Foard, M. (2014). *Causes and consequences of Chinese privet (Ligustrum sinense Lour.) invasion in hydrologically altered forested wetlands*: Arkansas State University.

Godfrey, R. K. (1988). *Trees, shrubs, and woody vines of northern Florida and adjacent Georgia and Alabama*: University of Georgia Press.

Gray, R. J. F. J. (1950). Chinese tallow, a four-way crop. *74*, 124.

Greene, B., & Blossey, B. (2014). Patterns of privet: urbanizing watersheds, invasive *Ligustrum sinense*, and performance of native plant species in Piedmont floodplain forests. *Ecosystems, 17*(6), 990-1001.

Guntenspergen, G. R., & Vairin, B. A. (1998). *Vulnerability of coastal wetlands in the Southeastern United States: climate change research results, 1992-97*: US Department of the Interior, US Geological Survey, National Wetlands ….

Hantson, W., Kooistra, L., & Slim, P. A. (2012). Mapping invasive woody species in coastal dunes in the N etherlands: a remote sensing approach using LIDAR and high‐resolution aerial photographs. *Applied vegetation science, 15*(4), 536-547.

Hawthorne, T., Elmore, V., Strong, A., Bennett-Martin, P., Finnie, J., Parkman, J., . . . Reed, J. (2015). Mapping non-native invasive species and accessibility in an urban forest: A case study of participatory mapping and citizen science in Atlanta, Georgia. *Applied Geography, 56*, 187-198.

Hood, W. G., & Naiman, R. (2000). Vulnerability of riparian zones to invasion by exotic vascular plants. *Plant ecology, 148*(1), 105-114.

Howes, F. (1949). The Chinese tallow tree (*Sapium sebiferum Roxb*.): a source of drying oil. *Kew Bulletin, 4*(4), 573-580.

Hudson, J. R., Hanula, J. L., & Horn, S. (2014). Impacts of removing Chinese privet from riparian forests on plant communities and tree growth five years later. *Forest Ecology and Management, 324*, 101-108.

Ill, E. W. R., Nelson, G. A., Sapkota, S. K., Seeger, E. B., & Martella, K. D. (2002). Mapping Chinese tallow with color-infrared photography. *Photogrammetric Engineering, 68*(3), 251-255.

Joshi, C., De Leeuw, J., & Van Duren, I. C. (2004). *Remote sensing and GIS applications for mapping and spatial modelling of invasive species.* Paper presented at the Proceedings of ISPRS.

Jubinsky, G., & Anderson, L. C. (1996). The invasive potential of Chinese tallow-tree (*Sapium sebiferum Roxb*.) in the southeast. *Castanea*, 226-231.

Kim, J., Popescu, S. C., Lopez, R. R., Wu, X. B., & Silvy, N. J. (2020). Vegetation mapping of No Name Key, Florida using lidar and multispectral remote sensing. *International Journal of Remote Sensing, 41*(24), 9469-9506.

Liang, W., Abidi, M., Carrasco, L., McNelis, J., Tran, L., Li, Y., & Grant, J. (2020). Mapping vegetation at species level with high-resolution multispectral and lidar data over a large spatial area: a case study with Kudzu. *Remote Sensing, 12*(4), 609.

Lockwood, J. L., Hoopes, M. F., & Marchetti, M. P. (2013). *Invasion ecology*: John Wiley & Sons.

Miller, J. H., Lemke, D., Coulston, J., Wear, D. N., & Greis, J. G. (2013). The invasion of southern forests by nonnative plants: current and future occupation, with impacts, management strategies, and mitigation approaches. *178*, 397-456.

Myers, R. K., & Van Lear, D. H. (1998). Hurricane-fire interactions in coastal forests of the south: a review and hypothesis. *Forest Ecology and Management, 103*(2-3), 265-276.

Nagendra, H., Lucas, R., Honrado, J. P., Jongman, R. H., Tarantino, C., Adamo, M., & Mairota, P. (2013). Remote sensing for conservation monitoring: Assessing protected areas, habitat extent, habitat condition, species diversity, and threats. *Ecological Indicators, 33*, 45-59.

Niphadkar, M., & Nagendra, H. (2016). Remote sensing of invasive plants: incorporating functional traits into the picture. *International Journal of Remote Sensing, 37*(13), 3074-3085.

Order, E. P. E. O. (1999). Invasive Species. *Fed. Regist., 64*, 6183–6186.

Pattison, R. R., & Mack, R. N. (2009). Environmental constraints on the invasion of *Triadica sebifera* in the eastern United States: an experimental field assessment. *Oecologia, 158*(4), 591-602.

Pile, L. S., Wang, G. G., Stovall, J. P., Siemann, E., Wheeler, G. S., & Gabler, C. A. (2017). Mechanisms of Chinese tallow (*Triadica sebifera*) invasion and their management implications–a review. *Forest Ecology and Management, 404*, 1-13.

Popescu, S. C. (2007). Estimating biomass of individual pine trees using airborne lidar. *Biomass and Bioenergy, 31*(9), 646-655.

Ramsey, E., & Rangoonwala, A. (2018). Hyperspectral remote sensing of wetland vegetation. In *Advanced Applications in Remote Sensing of Agricultural Crops and Natural Vegetation* (pp. 219-245): CRC Press.

Randall, J. P. (2015). *Remote-Sensing Detection of Invasive Chinese Tallow (Triadica sebifera) in a Floodplain Environment.* Texas A&M University,

Rogers, W. E., & Siemann, E. (2003). Effects of simulated herbivory and resources on Chinese tallow tree (*Sapium sebiferum, Euphorbiaceae*) invasion of native coastal prairie. *American Journal of Botany, 90*(2), 243-249.

Simberloff, D., Martin, J.-L., Genovesi, P., Maris, V., Wardle, D. A., Aronson, J., . . . Pascal, M. (2013). Impacts of biological invasions: what's what and the way forward. *Trends in ecology and evolution, 28*(1), 58-66.

Sui, Z. (2015). *Modeling tree species distribution and dynamics under a changing climate, natural disturbances, and harvest alternatives in the southern United States*: Mississippi State University.

Van Lear, D. H., Carroll, W., Kapeluck, P., & Johnson, R. (2005). History and restoration of the longleaf pine-grassland ecosystem: implications for species at risk. *Forest Ecology Management, 211*(1-2), 150-165.

Wang, H.-H. (2011). *Occupation, dispersal, and economic impact of major invasive plant species in southern US forests.* Texas A & M University,

Webster, C. R., Jenkins, M. A., & Jose, S. (2006). Woody invaders and the challenges they pose to forest ecosystems in the eastern United States. *Journal of Forestry, 104*(7), 366-374.

Wilcove, D. S., Rothstein, D., Dubow, J., Phillips, A., & Losos, E. (1998). Quantifying threats to imperiled species in the United States. *BioScience, 48*(8), 607-615.

Yang, S. (2019). Distribution and spread mechanisms of Chinese tallow (*Triadica sebifera*) at multiple spatial scales within forests in the southeastern United States.

Yang, S., Fan, Z., Liu, X., & Ezell, A. W. (2021). Predicting the spread of Chinese tallow (*Triadica sebifera*) in the southeastern United States forestland: Mechanism and risk factors at the regional scale. *Forest Ecology and Management, 482*, 118892.

Zedler, J. B., & Kercher, S. (2004). Causes and consequences of invasive plants in wetlands: opportunities, opportunists, and outcomes. *Critical Reviews in Plant Sciences, 23*(5), 431-452.

Zimmerman, R., Wetzel, R., Siemann, E., Reed, J., Miller, R. L., Harwell, M., . . . Twilley, R. (2001). Confronting climate change in the Gulf region: prospects for sustaining our ecological heritage.

Chapter 2: Mapping invasive *Triadica sebifera* (Chinese tallow) and *Ligustrum sinense* (Chinese privet) using NAIP imagery and airborne lidar in coastal Alabama, U.S.A.

2.1 Introduction

Invasive plant species are defined as species whose introduction causes or is likely to cause economic or environmental harm or harm to human health (Order, 1999). They impair soil nutrient cycling, and alter the forest stand structure (Ehrenfeld, 2010). In almost half of US ecosystems, the infestation of invasive plant species contribute significant threats to plant species listed under the Endangered Species Act (Wilcove et al., 1998). Invasive plant species have caused a decline of 42% of US endangered and threatened species (Order, 1999). In addition, the removal of invasive plant species is costly (Hobbs & Humphries, 1995). The annual cost of invasion related to ecological damages has increased from $2 billion in 1960-1969 to $ 21 billion in 2010- 2020 (Fantle-Lepczyk et al., 2022).

Several invasive species are well-established throughout forested regions of the US. Among the ten worst invasive plants in Alabama according to the Alabama Invasive Plant Council are, *Triadica sebifera* (Chinese tallow) and *Ligustrum sinense* (Chinese privet) (ALIPC, 2019). Both invasive plants are native to China and were introduced to the US in 1776 and 1852, respectively, for ornamental purposes. Chinese tallow is a deciduous tree that can grow up to 60 feet (18.3 m) high and 3 feet (0.9 m) wide at maturity. The main pathways for short-distance seed dispersal of Chinese tallow are water currents, long-distance seed dispersal facilitated by birds species that prefer seeds with high oil content, and large-scale disturbances such as hurricanes (Yang et al., 2021). Chinese tallow contains high tannins in the leaf litter, that alters the composition of microbial communities and eventually displaces native species (Montez et al., 2021). In the south-eastern US, from North Carolina south to Florida and west through Louisiana and Arkansas to Texas, Chinese tallow has invaded wet coastal areas and spread rapidly inland. Around 518 million dollars of timber loss is estimated within the next 20 years if no effective control measures for Chinese tallow is applied (Wang, 2011).

Chinese privet is a semi-evergreen to evergreen shrub that can grow up to 10 m (Miller et al., 2013). It colonizes by root sprouts, and seed dispersal is carried out by birds and wildlife. It has a negative impact on native plant abundance and diversity (Foard, 2014; Wilcox & Beck, 2007), limits forest regeneration (Cash et al., 2020; Loewenstein & Loewenstein, 2005), and

often produces a monoculture (Hart & Holmes, 2013). Furthermore, it has been implicated in the decline of species of conservation concern, such as the green pitcherplant (*Sarracenia oreophila*), and Schweinitz's sunflower (*Helianthus schweinitzii*) (Cash et al., 2020). Reported estimates for the cost to control Chinese privet range from $216–$1,820 per ha (Benez-Secanho et al., 2018; Klepac et al., 2007). Around 2.72 billion dollars of timber loss, within the next 20 years, is estimated if no effective control measures for Chinese privet is applied (Wang, 2011).

Coastal ecosystems are ecologically important and sensitive to the impact of climate change (Ng et al., 2021). They play a critical role in global climate and the carbon cycle by sequestering carbon (Heckbert et al., 2011). Coastal ecosystems and wetlands are especially vulnerable to invasive plant species because they interact with climate change (Zedler & Kercher, 2004). The invasive species can form monotypic stands and impact nutrient cycling in wetland ecosystems (Bush et al., 2020). The study of invasive species in the coastal areas can help understand the associated factors that facilitate the growth and spread of invasives in these and other areas. A primary step to understanding the trend and pattern of invasive species spread is the development of spatially comprehensive maps of distribution. This information provides essential support for decision-making for effective invasive species management that can moderate their spread.

Field surveys can be used to collect detailed information on invasive plant species; however, this approach often is not practical for large geographical areas because of labor, time, capital constraints, and difficulty in accessing remote areas of interest (Bradley, 2014; Ismail et al., 2016; Zuberi et al., 2014). On the other hand, remote sensing technologies have been increasingly used for invasive plant species detection and mapping due to the capability to provide synoptic views over large geographical extents (Huang & Asner, 2009) and acquire data over inaccessible remote areas (Matongera et al., 2018). Several studies have shown that using remotely sensed data to map invasive plants may be a viable option. Bradley (2014) explored spectral, textural and phenological approaches for remote detection of invasive plants. Ismail et al. (2016) found that the synergy of multisource remotely sensed data could increase image classification accuracy.

Many studies highlight higher accuracy in detection and vegetation mapping using lidar combined with high-resolution multispectral imagery (Asner, 2008; Kim et al., 2020; Liang et al., 2020). Asner et al. (2008) explained that lidar, when combined with imagery, was found to

detect woody invasive tree species such as *F. uhdei, P. cattleianum, M. faya* for studying the presence and abundance of species. The use of aerial imagery and lidar-derived products increases the potential for detecting invasive species, particularly for taller woody invasive species (Asner, 2008; Dubayah & Drake, 2000; Hantson et al., 2012; Kim et al., 2020; Liang et al., 2020; Popescu, 2007). For instance, Hantson et al. (2012) demonstrated that lidar-derived products using Maximum Likelihood classification increased the overall classification accuracy from 39% to 50% for woody invasive species. The use of aerial imagery alone underestimated the classification of shrub vegetation, but the integration of lidar and imagery helps distinguish shrub vegetation from tall trees (Bork & Su, 2007).

Image classification techniques like Iterative Self Organizing Data Analysis Technique (ISODATA) clustering (Ustin et al., 2002) and Maximum Likelihood classifier (Michez et al., 2016) are widely used to map invasive species. However, Maximum Likelihood supervised classifier failed to generate a landcover classification map with sufficient accuracy on repeated classification attempts (Hayes et al., 2014). Over the last two decades, machine learning algorithms have been widely used to classify invasive plant species and demonstrate the ability to obtain accurate and reliable information from satellite imagery. Among machine learning methods described in the literature, Random Forest (RF) is considered desirable for multisource classification of remote sensing data (Gislason et al., 2006). Several studies have demonstrated its superiority for high-dimensional input data such as hyperspectral imagery and multi-source data (Abdel-Rahman et al., 2014; Chan et al., 2012; Ham et al., 2005; Jensen et al., 2020; Shoot et al., 2021). Kim et al. (2020) conducted vegetation mapping with lidar and multispectral imagery using four different classification algorithms (Support Vector Machine, RF, Maximum Likelihood, and Mahalanobis Distance), and RF classification using NAIP-lidar stacked image provided the highest overall accuracy (75.7%).

A study on Chinese tallow mapping across a 48.25 km^2 coastal region of Texas-Louisiana showed classification accuracies greater than 95% at 0.5 m and 1 m spatial resolution using color-infrared photography (Ill et al., 2002). Authors used imagery collected during senescence when leaves of Chinese tallow were bright red, but observed that not all senescing tallow leaves were bright red. Another study conducted on the coastal region of southern U.S. observed an overall classification accuracy of 80% for mapping Chinese tallow using RF (Randall, 2015). The application of remote sensing data for mapping Chinese privet is limited. A study using

citizen science data showed 84% accuracy in mapping Chinese privet over a study area of 0.72 km^2 in Atlanta, Georgia (Hawthorne et al., 2015). They used Inverse Distance Weighted spatial interpolation techniques to interpolate the area covered by invasive species over the study area. Cash et al. (2020) used moderate resolution multispectral images (Landsat 8 and Sentinel 2) to map Chinese privet at a 10 m and 30 m spatial resolution over a 23 km^2 study site and obtained an overall accuracy of 92.3% using the Maximum Likelihood algorithm (Cash et al., 2020). This work highlights the utility of satellite imagery for detecting dense monocultures of Chinese privet with high accuracy.

Although previous studies have focused on mapping Chinese tallow (Ill et al., 2002; Ramsey & Rangoonwala, 2018) and Chinese privet (Barnett, 2016; Cash et al., 2020; Hawthorne et al., 2015) over a small spatial extent, the potential for the use of freely available remotely sensed data for mapping invasive species over large spatial extent has not been comprehensively investigated. Especially, there is a need to develop effective methods for detecting, and mapping the shrubs and understory invasive species (Joshi et al., 2004). More importantly, to date, there are not spatially explicit fine-scale maps of Chinese tallow and Chinese privet for coastal Alabama and Mississippi. The increasing availability of airborne lidar and NAIP imagery presents an exceptional convenience to achieve detailed, finer-scale observations for invasive species assessments.

The overall goal of this study was to develop the most accurate and high-resolution distribution map of *Triadica sebifera* and *Ligustrum sinense*, among the image classification approaches used, in the coastal region of Alabama and Mississippi. With a focus on three study sites, Bon Secour National Wildlife Refuge, Mobile Tensaw Management Area, and Mississippi Sandhill Crane National Wildlife Refuge. The specific objectives were to:

1. Determine the extent and coverage of Chinese tallow and Chinese privet.
2. Identify the most accurate approach for developing mapped products of Chinese tallow and Chinese privet.

2.2 Materials and Methods

To meet the study's overall goal, remotely sensed and field inventory data were used. Remotely sensed data are NAIP imagery and lidar. Vegetation indexes such as Normalized Difference Vegetation Index (NDVI) derived from NAIP imagery were used for differentiating

vegetation from non-vegetation. Variables such as a Canopy Height Model (CHM) and Canopy Density Model (CDM) derived from lidar, were used to improve invasives' detection accuracy. Bands of NAIP imagery were integrated with lidar-derived variables for the image classification. The workflow used for the study is shown in Figure 1.

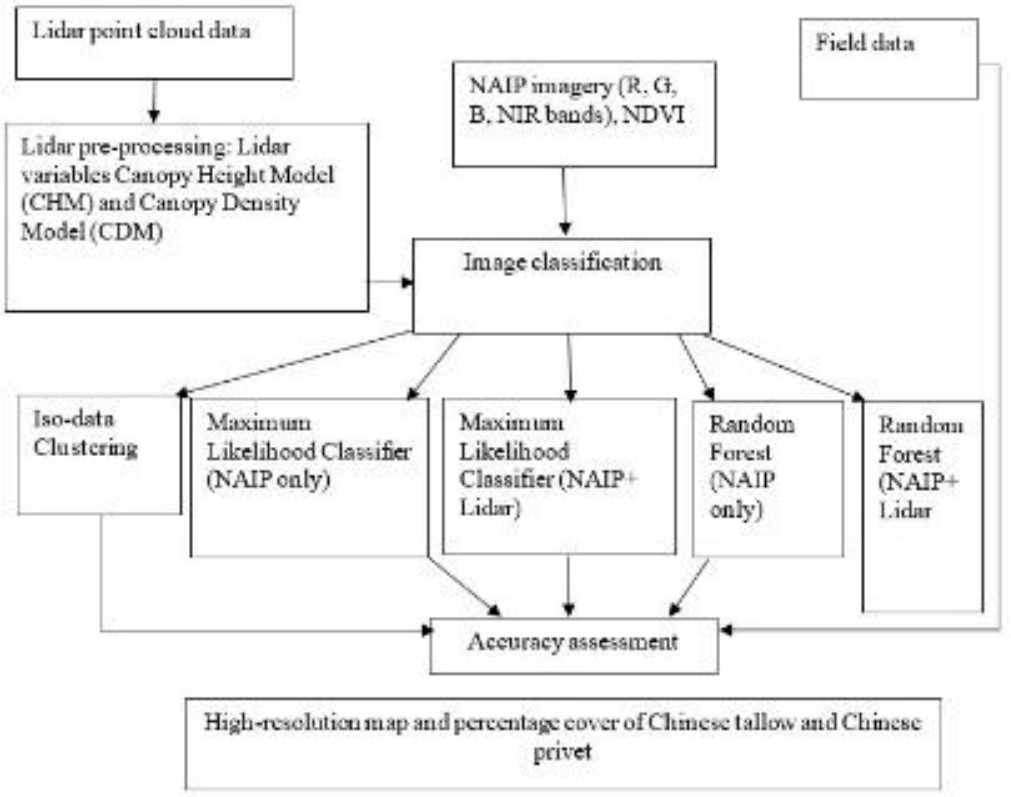

Figure 1. Workflow of the first study.

2.2.1 Study area

The study was carried out within Bon Secour National Wildlife Refuge, Mobile Tensaw Wildlife Management Area and Mississippi Sandhill Crane National Wildlife Refuge located in the coastal region of southern US (Figure 2). Specifically, Bon Secour National Wildlife Refuge and Mobile Tensaw Wildlife Management Area are located in Alabama. Southern Alabama is classified as a humid subtropical climate with an average annual temperature of 18 °C (64 °F). The temperature in the hottest month (July) and coldest month (January) averages 32 °C (90 °F) and 4°C (40°F), respectively. The region's average annual precipitation is 1,400 mm (56 inches). The landforms of coastal Alabama consist of flat plains, marshes, river deltas, and wetlands. Bon Secour is located within the Gulf Shores region of Alabama and covers an area of 20.03 km². The area is dominated by pine forests, hardwood forests, mixed pine and hardwood forests, wetlands, and marshlands. The landscape is flat, and waterlogged all year round, on some areas. Mobile Tensaw is located in Baldwin and Mobile counties, covering an area of 751 km² and consist of bottomland hardwoods, swamp lands, bogs, marshes, waterways of rivers, creeks, sloughs, ponds, and lakes. This area is dominated by longleaf-slash pine (*Pinus palustris* and *Pinus elliottii*), oak-pine (*Quercus spp.* and *Pinus spp.*), oak- gum cypress (*Quercus spp.*, *Nyssa spp*. and *Taxodium spp.*).

The Mississippi Sandhill Crane National Wildlife Refuge is in Mississippi (Figure 2). Wet pine savanna, herbaceous species, grasses, and shrubs under pine and hardwood trees, predominates the wildlife refuge. One of 99 burn units from the west block of the Wildlife Refuge, having an area of 4.75 km^2, was used for the study.

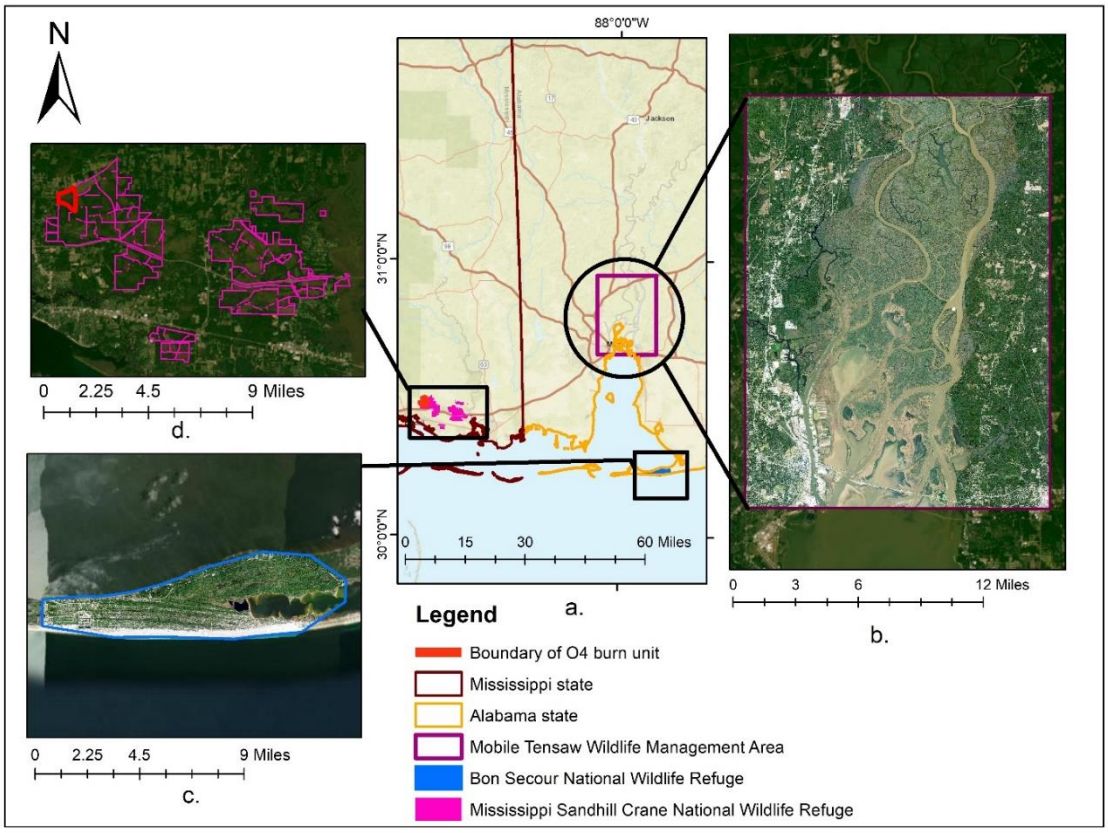

Figure 2. Map of the study area, showing. a. Mississippi and Alabama with the location of three study sites. b. Mobile Tensaw Wildlife Management Area. c. Bon Secour National Wildlife Refuge. d. Mississippi Sandhill Crane National Wildlife Refuge with the boundary of O4 burn unit in it.

2.2.2 Datasets

2.2.2.1 Field data

Field data collection was carried out in May 2021, along the road networks of Bon Secour and Mobile Tensaw area, for ground truthing. Both the study sites contain large expanses of bottomland forest and marshy areas that remain wet for much of the year. As a result, much of the area is, for the most part, inaccessible. Therefore, field data collection was limited to along the road networks. Area. Much of the area adjacent to roads in the area was private property, which had limited access. As a result, only 99 field locations for Chinese tallow and 48 field locations for Chinese privet were recorded. These recorded presence and absence information of the invasives were used to validate the accuracy of the mapped products. Only Chinese tallow occurred on Bon Secour National Wildlife Refuge, while both Chinese tallow and Chinese privet were observed on Mobile Tensaw Wildlife Management Area. Hence, the distribution map prepared for Bon Secour National Wildlife Refuge was just for Chinese tallow. The distribution map prepared for the Mobile Tensaw Wildlife Management Area was for both Chinese tallow and Chinese privet.

2.2.2.2 Remote Sensing Data

Freely available remotely sensed data were used for the study. Three different sources of remotely sensed data were used, i.e., NAIP imagery, Digital Elevation Model (DEM), and discrete return lidar data. NAIP imagery is acquired every three years during the agricultural growing seasons. The principal purpose of the NAIP program is to make aerial imagery available within a year of acquisition. NAIP imagery with the datum of NAD 1983 and in the UTM zone 16 acquired between 2019 and 2020 covering the study area was downloaded from the United States Geological Survey (USGS) Earth Explorer (U.S. Geological Survey, 2019a). The image has a spatial resolution of 1 m and spectral resolution of four bands (RGB and Near Infrared). DEMs from 2014 to 2018 were downloaded for two study sites from United States Geological Survey (USGS) Earth Explorer.

Airborne lidar point clouds for the study area were accessed from USGS 3DEP. The primary goal of USGS 3DEP is to acquire nationwide lidar data and offer the first-ever national baseline of reliable high-resolution 3D point cloud data (United States Geological Survey,

2019b). Discrete return lidar data from 2015 to 2020 for the two study sites were used. Based on availability, lidar data acquired in 2017 was downloaded for Bon Secour, and lidar data collected in 2015 and 2019 were retrieved for Mobile Tensaw area. The lidar data has Quality level 2 (QL2), and the point density for each lidar tile is less than 3 points per m^2 with the lidar tiles that were already classified into classes such as ground, vegetation, and noises.

2.2.2.3 NAIP pre-processing and derived products

Five and 30 NAIP image tiles were downloaded for Bon Secour and Mobile Tensaw area, respectively. Image tiles were pre-processed in 2 steps. At first, a single image mosaic was prepared from the multiple images using mosaic tool in ArcGIS Desktop software. The second step in NAIP pre-processing was clipping the mosaicked image to the extent of the study area using clip tool in ArcGIS Desktop software.

Four bands of pre-processed NAIP imagery (blue, green, red and near infrared) were used for image classification. A band represents recorded energy having specific wavelength of electromagnetic spectrum. Also, NDVI derived from NAIP using Environment for Visualizing Images (ENVI) software was used for image classification. NDVI is a vegetation index with values ranging from -1 to +1, to indicate healthy green vegetation. The value closer to +1 represents healthy vegetation, and the value closer to 0 represents lower or no vegetation.

2.2.2.4 Lidar data processing and derived products

The lidar point cloud data were pre-processed to remove noise returns and derive heights above ground level or normalized heights using LAStools (Isenburg, 2014) and ArcGIS. Some of the lidar data were originally collected in Alabama State Plane West Zone (unit: feet) coordinate system, but it was converted to NAD83 UTM zone 16 N (unit: meter) for consistency with NAIP imagery. The points were normalized using lasheight tool from LAStools, and filtering was done to remove heights below 0 m and above 40 m, so that height of desired range could be accessed. The height cut-off was defined based on the tallest tree recorded on the study site, i.e., 39.9 meters. Then, lasclip tool from LAStools was used to extract all returns of lidar data within the study area.

A 1-meter Canopy Height Model (CHM) was derived from the height-normalized data. A Digital Surface Model (DSM) was derived using first returns from the lidar point cloud. Then, the CHM was generated by subtracting the DEM from DSM. A lidar-derived Canopy Density

Model (CDM) was then obtained using lascanopy tool from LAStools. The height cut-offs of 7 m, and 40 m were used while creating the CDM. Height under 7 m referred to a shrub, and (0 - 40) m referred to all vegetation, including Chinese tallow and Chinese privet. All returns between the height cut-off of (0 - 40) m were used for generating the overall CDM. Furthermore, all returns within the height cut-offs under 7 m were used to generate CDM, especially for Chinese privet detection.

2.2.3 Training data

Two sets of data, i.e, training data and test data, were defined based on the training data selection guideline from Fundamentals of Remote Sensing (Chuvieco, 2016). The training data was used to train the classifiers for supervised classification and the test data was used to validate the mapped products using ground truth. Around 4-8 Regions of Interest (ROIs) for each class were selected separately. The ROIs for training data were selected using the visual interpretation based on the known locations of the classes and separate ROIs for test data were selected based on the ground truth. The ROIs were selected in such a way that they capture spectral variability and is a representative sample of the class. ROIs selection for invasive plants was carried out using remotely sensed data and field data. Visual interpretation using aerial imagery and Google Earth was done to distinguish the invasive species from other vegetation based on known locations from field visits. Jeffries-Matusita distance and Transformed Divergence measure, scaled between 0 and 2 (Sen et al., 2019), were used to access the spectral separability of the classes. The spectral separability of classes prepared for training and test datasets was greater than 1.9, indicating higher spectral separability of classes.

2.2.4 Image classification

The image classification was carried out using two datasets. First, using the NAIP imagery alone and second, integrating the spectral bands from the NAIP imagery and lidar-derived canopy height and cover model. These lidar-derived products were resampled to match that of NAIP imagery and stacked for image classification. Three image classification approaches were carried out using both datasets. ISODATA clustering, as a representation of unsupervised classifier, Maximum Likelihood classifier, as a representation of supervised classifier (Ahmad & Quegan, 2013) and RF, as a representation of non-parametric machine learning algorithm were implemented. Unsupervised classifiers group the pixels with common

characteristics based on software analysis of image without the user's knowledge. However, supervised classifiers use the representative sample pixels of specific classes provided by the training pixels to classify all other pixels in the image. The RF algorithm learns the relationship between predictor and response data (Horning, 2010) and derives prediction from decision trees to provide reliable classification (Breiman, 2001).

First image classification approach was ISODATA clustering. Based on the cluster of pixels that share similar spectral properties, a total of 15 color-coded classes were prepared with five iterations. After that, post classification was done to refine and reduce the number of classes using image interpretation. Each class was closely examined using the classified and original imagery and the classes that share similar spectral property were combined to form six classes of water, built-up, coastal sand, other vegetation, Chinese tallow, and Chinese privet for Mobile Tensaw area. The classes such as water, built-up, coastal sand, other vegetation were then merged into a single class named as other. Finally, a total of three classes: Chinese tallow, Chinese privet and other (water, built-up, coastal sand, other vegetation) were prepared. For Bon Secour National Wildlife Refuge, post classification was done on 15 color coded classes prepared with five iterations to form five classes of water, built-up, coastal sand, other vegetation, and Chinese tallow. The classes such as water, built-up, coastal sand, other vegetation were then merged into a single class named as other. At last, a total of two classes: Chinese tallow and other were obtained for better representative distribution of Chinese tallow.

Second image classification approach was Maximum Likelihood classifier. It requires training data (Section 2.3) based on the known location of classes. The classifier assigns pixels to classes based on spectral properties of the training data. For Mobile Tensaw area, six ROIs (water, built-up, coastal sand, other vegetation, Chinese tallow, and Chinese privet) were prepared separately for training and test data (Section 2.3) using ROI tool of ENVI. While acquiring ROIs, NAIP imagery was zoomed so that the desired pixels of the ROIs can be recorded. The unimodal statistics of ROIs having spectral separability (Section 2.3) greater than 1.9 was obtained. The ROIs such as water, built-up, coastal sand, other vegetation were then merged into a single ROI named other and three classes: Chinese tallow, Chinese privet, and other were obtained. For Bon Secour area, five ROIs (water, built-up, coastal sand, other vegetation, and Chinese tallow) were initially prepared. The ROIs such as water, built-up, coastal

sand, other vegetation were then merged into a single ROI named other and finally two classes: Chinese tallow and other were obtained.

Third image classification approach was RF. RF was done using ModelMap. ModelMap is a R package that allows for user-friendly modeling and mapping over vast geographic areas using R functions like model.build(), model.diagnostics(), and model.mapmake() (Freeman et al., 2009). The categorical response variable and predictor variables were defined as demonstrated by (Freeman & Frescino, 2018). Landcover classification map prepared using the Maximum Likelihood classifier was used as a categorical response variable. Predictor variables used for RF were bands of NAIP imagery (red, green, blue, and infrared), vegetation index derived from NAIP imagery (NDVI), and lidar-derived variables (CHM, CDM).

2.2.5 Accuracy assessment

The classification accuracy of NAIP and NAIP-lidar stacked image were assessed using confusion matrices in the ENVI software. The separate test data, created using presence and absence information from ground truth, was used to assess the accuracy of each classification approach used for the study. The overall classification accuracy was estimated by calculating the proportion of correctly classified pixels of the land cover classes out of the total pixels in the classified image. Along with the overall classification accuracy, the Kappa coefficient was also estimated. The Kappa coefficient indicates how much better an image classification is compared to a random chance assignment of the pixels into each land cover class (Congalton & Green, 2019). The confusion matrix created had information about the correctly classified pixels for each land cover class and the pixels that were mistakenly classified as other land cover classes. Producer's accuracy (PA), User's accuracy (UA), omission error and commission error for each of the land cover classes were also reported. Omission errors are where pixels that belong to the ground truth class were not placed in the correct class. Commission errors are expressed as the pixels that are part of another class classified as belonging to the class of interest.

Based on the confusion matrix, PA, UA, omission error, and commission error of mapping Chinese tallow and Chinese privet were assessed.

2.3 Results

Three image classification approaches (ISODATA clustering, Maximum Likelihood classifier, and Random Forest) were implemented. For ISODATA clustering, only NAIP

imagery was used for classification. Two different input datasets (NAIP imagery alone and NAIP imagery integrated with lidar-derived variables) were used for Maximum Likelihood classifier and Random Forest. Results were summarized separately based on the dataset used. At first, the classification accuracies obtained using NAIP imagery alone were presented followed by the classification accuracies obtained using NAIP imagery and lidar-derived variables for each study site. In addition to that, tables represent comparison of results obtained from the accuracy assessment including overall accuracy, kappa coefficient, producer's accuracy, and user's accuracy. Figures represent the distribution of Chinese tallow and Chinese privet produced with maximum overall accuracy using specific dataset among the image classification approaches used. Confusion matrix using ground truth ROIs was used to conduct accuracy assessment. The matrix contained detailed information of each image classification including the correctly classified pixels and pixels confused with the specific classes. In general, grassland, shrubs, and algal concentration found in both study areas were confused with trees due to the similar spectral reflectance.

2.3.1. Mobile Tensaw Wildlife Management Area

2.3.1.1 Assessment of classification accuracies using NAIP imagery

The overall accuracy (64.77%) and kappa coefficient (0.55) of the classification map using ISODATA classifier increased to 74.73% and 0.67 respectively using the Maximum Likelihood classifier on NAIP imagery (Table 1). The overall accuracy further increased from 74.73% to 79.58% using Random Forest on NAIP imagery. But the kappa coefficient obtained with Random Forest (0.34) is lower than the kappa coefficient obtained with Maximum Likelihood classifier (0.67). The maximum PA (100%) for classifying Chinese tallow and Chinese privet was obtained with Maximum Likelihood classifier. Although ISODATA classification yielded a lower overall accuracy, the maximum UA (95.85%) for classifying Chinese tallow and maximum UA (88.89%) for classifying Chinese privet was produced from the ISODATA algorithm, as shown in Table 1.

Table 1. Comparison of accuracies obtained using NAIP imagery alone for Mobile Tensaw Wildlife Management Area based on three different image classification approaches.

	ISODATA	Maximum Likelihood	Random Forest
Overall Accuracy (%)	64.77	74.73	79.58
Kappa Coefficient	0.55	0.67	0.34
Producer's Accuracy for Chinese tallow (%)	93.91	100	15.91
User's Accuracy for Chinese tallow (%)	95.85	80	53.85
Producer's Accuracy for Chinese privet (%)	13.56	100	0
User's Accuracy for Chinese privet (%)	88.89	70.83	0

The maximum overall accuracy 79.58% and kappa coefficient 0.34 was obtained using RF on NAIP imagery for Mobile Tensaw area (Figure 3).

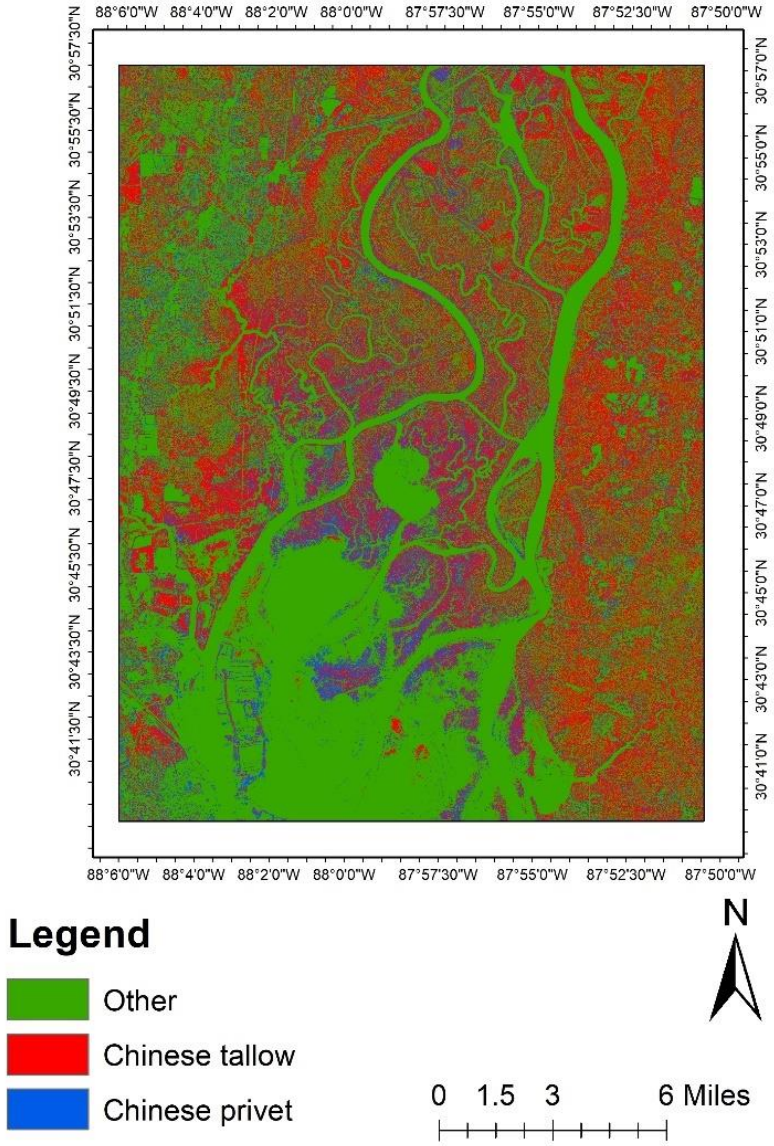

Figure 3. Map of Mobile Tensaw Wildlife Management Area showing the image classification results for the distribution of Chinese tallow and Chinese privet. The green area represents other (water, built-up, coastal sand, other vegetation such as hardwood and pine), red area represents the distribution of Chinese tallow and blue area represents the distribution of Chinese privet. The image shows the distribution map of Chinese tallow and Chinese privet using RF on NAIP imagery. This mapping approach has highest overall accuracy for classifying Chinese tallow and Chinese privet among the classification approaches using NAIP imagery alone.

Although the highest overall accuracy was obtained with RF using NAIP imagery alone for Mobile Tensaw Wildlife Management Area, the producer's accuracies and user's accuracies for Chinese tallow and Chinese privet were comparatively low as compared to other classification methods. The producer's accuracy for Chinese tallow was 15.91% (Table 3) and the user's accuracy for Chinese tallow was 53.85%. The method and dataset used could not detect Chinese privet. The confusion matrix shows that Chinese tallow had 88 ground truth pixels, 14 of those are correctly classified as Chinese tallow (Table 2). Hence, the producer's accuracy is 14/88=15.91%, which means 15.91% of time Chinese tallow was labelled as Chinese tallow on the classified image. Chinese tallow had a total of 26 classified pixels, 14 out of those classified pixels were classified correctly as Chinese tallow (Table 2). Hence, the user's accuracy is 14/26= 53.85%, which means that 53.85% of the area in classified image labelled as Chinese tallow (classified as Chinese tallow) was Chinese tallow on the ground. Similarly, Chinese privet has 34 ground truth pixels and a total of 116 pixels were classified as Chinese privet. Out of these classified pixels, none of the pixels were classified as Chinese privet.

Table 2. Confusion matrix obtained for RF using NAIP imagery alone for Mobile Tensaw Wildlife Management Area (in pixels).

Ground Truth (Pixels)				
Class	Chinese tallow	Chinese privet	Other	Total
Chinese tallow classified	14	11	1	26
Chinese privet classified	74	0	42	116
Other classified	0	23	575	598
Total	88	34	618	740

Table 3. Confusion matrix for RF using NAIP imagery alone for Mobile Tensaw Wildlife Management Area (in percent).

Ground Truth (Percent)				
Class	Chinese tallow	Chinese privet	Other	Total

Chinese tallow classified	15.91	32.35	0.16	3.51
Chinese privet classified	84.09	0	6.8	15.68
Other classified	0	67.65	93.04	80.81
Total	100	100	100	100

2.3.1.2 Assessment of classification accuracies using NAIP imagery and lidar-derived variables

The maximum overall accuracy (98.62%) and kappa coefficient (0.86) was obtained using Random Forest after adding lidar-derived CHM and CDM for privet to NAIP image bands (Table 4). Among the Maximum Likelihood classifiers used with NAIP imagery and different combination of lidar-derived variables, the maximum overall accuracy (83.24%) and kappa coefficient (0.79) was obtained using the CHM integrated with NAIP imagery. With the same input dataset and classification approach, the maximum UA (94.81%) for classifying Chinese tallow and the maximum PA (100%) for classifying Chinese privet was obtained. The maximum PA (97.73%) for classifying Chinese tallow was obtained with Maximum Likelihood classifier using the CHM and CDM for Chinese tallow integrated with NAIP imagery. The maximum UA (87.50%) for classifying Chinese privet was obtained with Maximum Likelihood classifier using the CHM and CDM for Chinese privet integrated with NAIP imagery (Table 4).

The maximum overall accuracy of 98.62% and kappa coefficient of 0.86 was obtained for RF using CHM and CDM for privet integrated with the NAIP imagery for Mobile Tensaw area (Figure 4).

Table 4. Comparison of accuracies obtained using NAIP imagery and lidar-derived variables for Mobile Tensaw Wildlife Management Area based on 3 different classification approaches.

	Maximum Likelihood (NAIP+ CHM)	Maximum Likelihood (NAIP+ CHM+ CDM for tallow)	Maximum Likelihood (NAIP+ CHM+ CDM for privet)	RF (NAIP +CHM)	RF (NAIP + CHM + CDM for tallow)	RF (NAIP + CHM + CDM for privet)
Overall Accuracy (%)	83.24	76.7	81.48	81.62	81.62	98.62
Kappa Coefficient	0.79	0.70	0.76	0.41	0.40	0.86
Producer's Accuracy for Chinese tallow (%)	82.95	97.73	-	14.77	15.91	-
User's Accuracy for Chinese tallow (%)	94.81	88.66	-	28.89	34.15	-
Producer's Accuracy for Chinese privet (%)	100	96.43	61.76	0	0	88.24
User's Accuracy for Chinese privet (%)	48.57	62.79	87.50	0	0	85.71

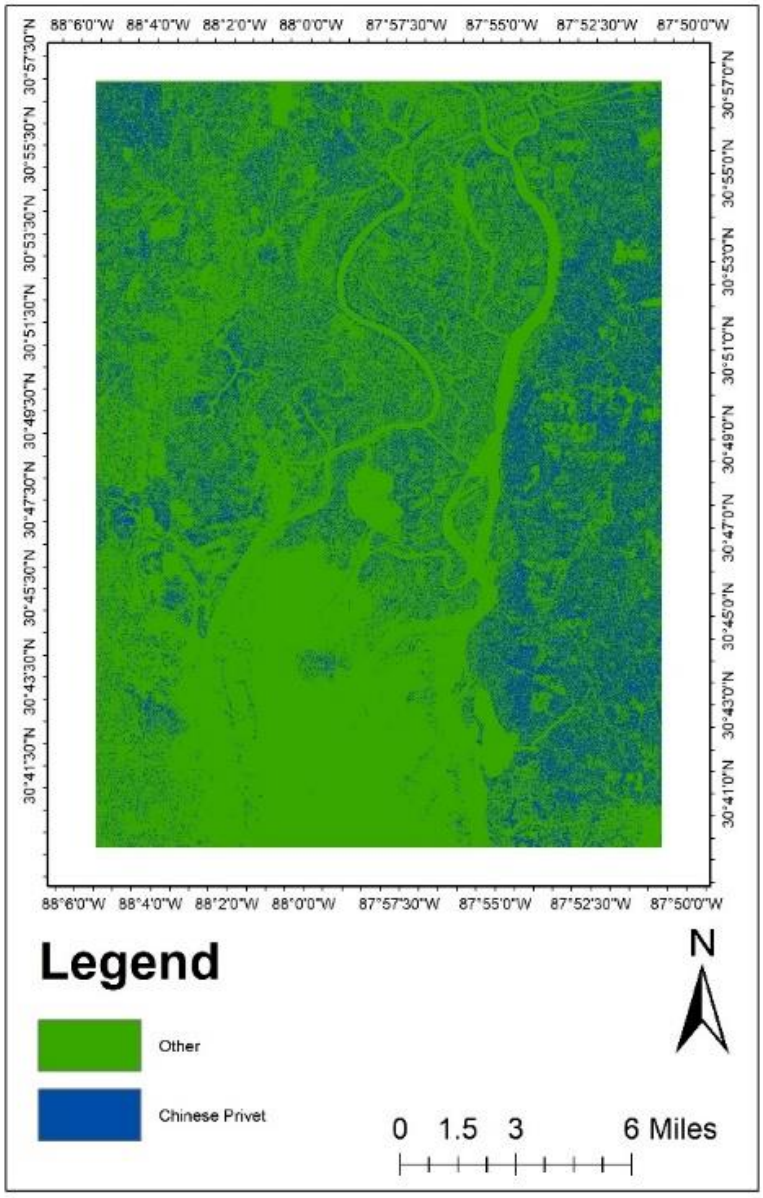

Figure 4. Map of Mobile Tensaw Wildlife Management Area showing the image classification results for the distribution of Chinese privet. The green area represents other (water, built-up, coastal sand, other vegetation such as hardwood and pine), and blue area represents the distribution of Chinese privet. Distribution map of Chinese privet using RF on the CHM and CDM for Chinese privet integrated with NAIP imagery. This mapping approach has highest overall accuracy for classifying Chinese privet.

The same method and dataset that produced highest overall accuracy and kappa coefficient gave good producer's accuracies and user's accuracies for classifying Chinese privet on Mobile Tensaw Wildlife Management Area. The producer's accuracy for Chinese privet was 88.24% (Table 6) and the user's accuracy for Chinese privet was 85.71%. The confusion matrix shows that Chinese privet had 34 ground truth pixels, 30 out of those are correctly classified as Chinese privet (Table 5). Hence, the producer's accuracy is 30/34=88.24%, which means 88.24% of time Chinese privet was labelled as Chinese privet on the classified image. Chinese privet had a total of 35 classified pixels, 30 out of those classified pixels were classified correctly as Chinese privet (Table 5). Hence, the user's accuracy is 30/35= 85.71%, which means that 85.71% of the area in classified image labelled as Chinese privet (classified as Chinese privet) was Chinese privet on the ground.

Table 5. Confusion matrix obtained using RF on the CHM and CDM for Chinese privet integrated with NAIP imagery for Mobile Tensaw Wildlife Management Area (in pixels).

Ground Truth (Pixels)			
Class	Other	Privet	Total
Other classified	613	4	617
Chinese privet classified	5	30	35
Total	618	34	652

Table 6. Confusion matrix obtained using RF on the CHM and CDM for Chinese privet integrated with NAIP imagery for Mobile Tensaw Wildlife Management Area (in percent).

Ground Truth (Percent)			
Class	Other	Privet	Total
Other classified	99.19	11.76	94.63
Chinese privet classified	0.81	88.24	5.37
Total	100	100	100

2.3.2. Bon Secour National Wildlife Refuge

2.3.2.1 Assessment of classification accuracies using NAIP imagery

The overall accuracy (83.58%) and kappa coefficient (0.68) of the classification map using ISODATA classifier increased to 98.5% and 0.97 respectively using the Maximum Likelihood classifier on NAIP imagery (Table 7). The overall accuracy (94.5%) and kappa coefficient (0.88) was obtained with Random Forest using NAIP imagery. The Maximum Likelihood classifier carried out on NAIP imagery produced the classification map with highest PA (97.14%) and UA (100%) for classifying Chinese tallow (Table 7). The maximum overall accuracy 98.5% and kappa coefficient 0.97 was obtained using Maximum Likelihood classifier on NAIP imagery for Bon Secour area (Figure 5).

Table 7. Table showing comparison of accuracies obtained using NAIP imagery alone for Bon Secour National Wildlife Refuge.

	ISODATA	Maximum Likelihood	Random Forest
Overall Accuracy (%)	83.58	98.5	94.5
Kappa Coefficient	0.68	0.97	0.88
Producer's Accuracy for Chinese tallow (%)	71.30	97.14	96.19
User's Accuracy for Chinese tallow (%)	100	100	93.52

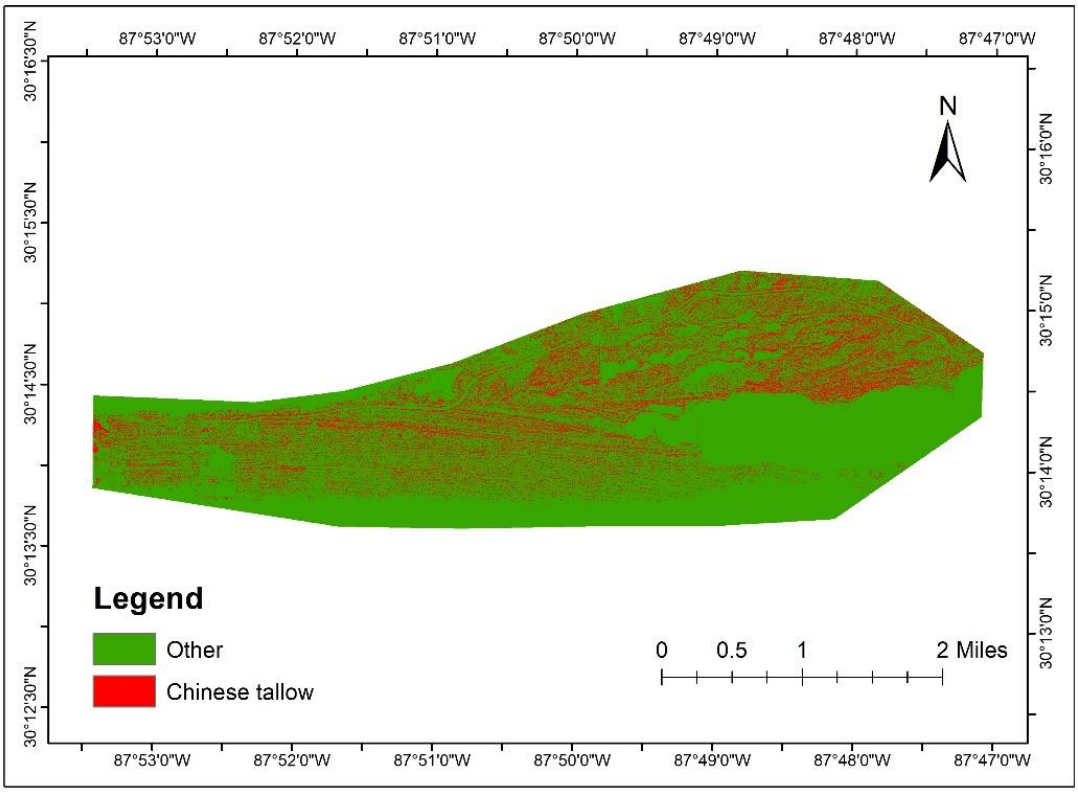

Figure 5. Map of Bon Secour National Wildlife Reserve showing the distribution of Chinese tallow produced for the Bon Secour area. The green area represents other (water, built-up, coastal sand, other vegetation such as hardwood and pine) and red area represents the distribution of Chinese tallow. The figure shows distribution map of Chinese tallow using Maximum Likelihood classifier on NAIP imagery alone. This mapping approach has highest overall accuracy for classifying Chinese tallow among the classification approaches using NAIP imagery alone.

The same method and dataset that produced highest overall accuracy and kappa coefficient gave good producer's accuracies and user's accuracies for classifying Chinese tallow on Bon Secour National Wildlife Reserve. The producer's accuracy for Chinese tallow was 97.14% (Table 9) and the user's accuracy was 100%. The confusion matrix shows that Chinese tallow had 105 ground truth pixels, 102 out of those are correctly classified as Chinese tallow (Table 8). Hence, the producer's accuracy is 102/105=97.14%, which means 97.14% of time Chinese tallow was labelled as Chinese tallow on the classified image. Chinese tallow had a total of 102 classified pixels, all those classified pixels were classified correctly as Chinese tallow (Table 8). Hence, the user's accuracy is 102/102= 100%, which means that 100% of the area in classified image labelled as Chinese tallow (classified as Chinese tallow) was Chinese tallow on the ground.

Table 8. Confusion matrix obtained for maximum likelihood classifier using NAIP imagery alone for Bon Secour National Wildlife Reserve (in pixels).

Ground Truth (Pixels)			
Class	Other	Chinese tallow	Total
Other classified	95	3	98
Chinese tallow classified	0	102	102
Total	95	105	200

Table 9. Confusion matrix obtained for maximum likelihood classifier using NAIP imagery alone for Bon Secour National Wildlife Refuge (in percent)

Ground Truth (Percent)			
Class	Other	Chinese tallow	Total
Other classified	100	2.86	49
Chinese tallow classified	0	97.14	51
Total	100	100	100

2.3.2.2 Assessment of classification accuracies using NAIP imagery and lidar-derived variables

The maximum overall accuracy (98.7%) and kappa coefficient (0.97) was obtained with Maximum Likelihood classifier using the lidar-derived CHM integrated with NAIP imagery (Table 10). The maximum PA (99.13%) and UA (100%) for classifying Chinese tallow was obtained with Random Forest using lidar-derived CHM and CDM integrated with NAIP imagery (Table 10). The maximum overall accuracy of 98.7% and kappa coefficient of 0.97 was obtained using NAIP imagery and lidar-derived variables for Bon Secour area (Figure 6).

Table 10. Table showing comparison of accuracies obtained using NAIP imagery and lidar-derived variables for Bon Secour National Wildlife Refuge.

	Maximum Likelihood (NAIP +CHM)	Maximum Likelihood (NAIP + CHM + CDM)	RF (NAIP +CHM)	RF (NAIP + CHM+ CDM)
Overall Accuracy (%)	98.77	89.52	94.29	95.23
Kappa Coefficient	0.97	0.79	0.88	0.90
Producer's Accuracy for Chinese tallow (%)	97.70	88.7	98.26	99.13
User's Accuracy for Chinese tallow (%)	100	100	99.12	100

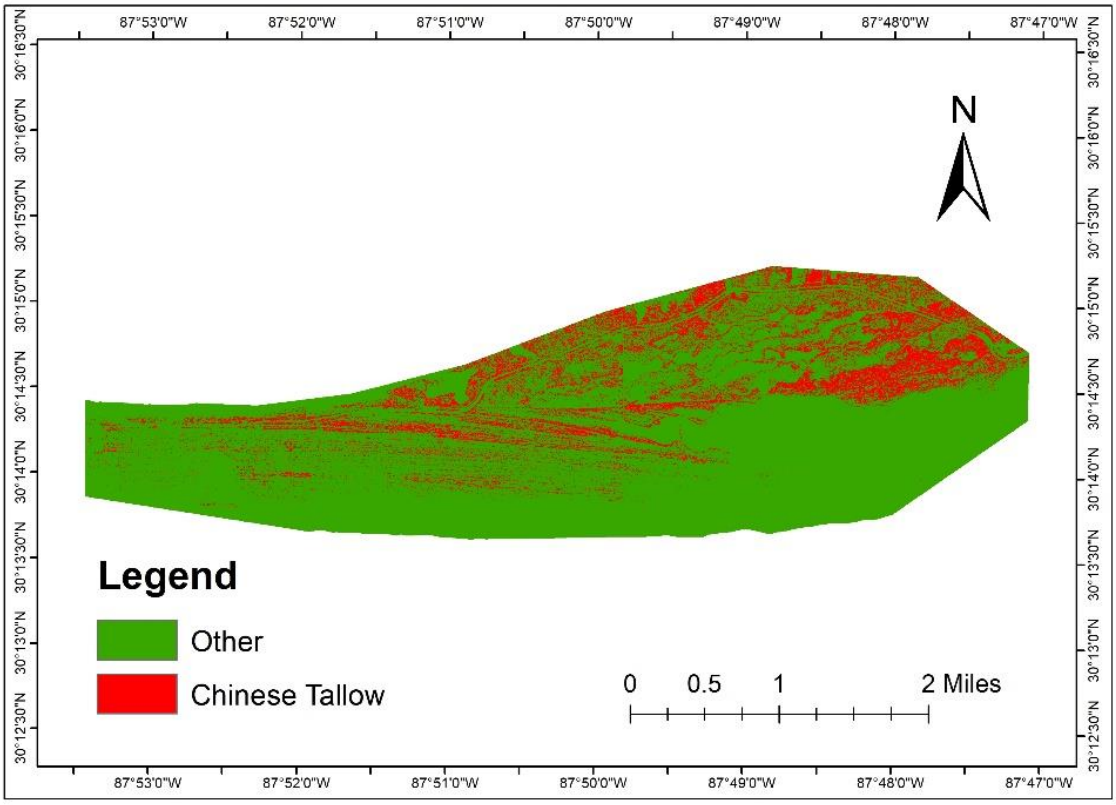

Figure 6. Map of Bon Secour National Wildlife Reserve showing the distribution of Chinese tallow produced for the Bon Secour site using Maximum Likelihood classifier on NAIP imagery integrated with lidar-derived variables. The green area represents other (water, built-up, coastal sand, other vegetation such as hardwood and pine) and red area represents the distribution of Chinese tallow. This mapping approach had the highest overall accuracy for classifying Chinese tallow among the classification approaches using NAIP imagery integrated with lidar-derived variables.

The same method and dataset that produced highest overall accuracy and kappa coefficient gave good producer's accuracies and user's accuracies for classifying Chinese tallow on Bon Secour National Wildlife Reserve. The producer's accuracy for Chinese tallow was 97.7% (Table 12) and the user's accuracy was 100%. The confusion matrix shows that of the 217 ground truth pixels for Chinese tallow, 212 were correctly classified as Chinese tallow (Table 11). Hence, the producer's accuracy is 212/217=97.7%, which means 97.7% of time Chinese tallow was labelled as Chinese tallow on the classified image. Chinese tallow had a total of 212 classified pixels, all those classified pixels were classified correctly as Chinese tallow (Table 11). Hence, the user's accuracy is 212/212= 100%, which means that 100% of the area in classified image labelled as Chinese tallow (classified as Chinese tallow) was Chinese tallow on the ground.

Table 11. Confusion matrix obtained for maximum likelihood classifier using NAIP imagery and lidar-derived variables for Bon Secour National Wildlife Refuge (in pixels).

Ground Truth (Pixels)			
Class	Other	Chinese tallow	Total
Other classified	189	5	194
Chinese tallow classified	0	212	212
Total	189	217	406

Table 12. Confusion matrix obtained for maximum likelihood classifier using NAIP imagery and lidar derived variables for Bon Secour National Wildlife Refuge (in percent).

Ground Truth (Percent)			
Class	Other	Chinese tallow	Total
Other classified	100	2.86	49
Chinese tallow classified	0	97.7	51
Total	100	100	100

2.3.3 Mississippi Sandhill Crane National Wildlife Refuge

2.3.3.1. Comparison of classification accuracies using NAIP imagery alone and NAIP imagery integrated with CHM

The overall accuracy (90.71%) and kappa coefficient (0.76) of the classification map using ISODATA classifier increased to 94.69% and 0.86 respectively using the Maximum Likelihood classifier on NAIP imagery (Table 13). The overall accuracy further increased to 96.63% and kappa coefficient increased to 0.92 after adding CHM to NAIP imagery using Maximum Likelihood classifier. The Maximum Likelihood classifier carried out on NAIP imagery and CHM produced the classification map with highest PA (94.61%) and UA (100%) for classifying Chinese tallow (Table 13). The maximum overall accuracy 96.63% and kappa coefficient 0.92 was obtained using Maximum Likelihood classifier on NAIP imagery and CHM for O4 burn unit of Mississippi Sandhill Crane National Wildlife Refuge area (Figure 7).

Table 13. Comparison of classification accuracies using NAIP imagery alone and NAIP imagery integrated with CHM for O4 burn unit of Mississippi Sandhill Crane National Wildlife Refuge.

	ISODATA (NAIP only)	Maximum Likelihood (NAIP only)	Maximum Likelihood (NAIP+CHM)
Overall Accuracy (%)	90.71	94.69	96.63
Kappa Coefficient	0.76	0.86	0.92
Producer's Accuracy for Chinese tallow (%)	69.57	82.61	94.61
User's Accuracy for Chinese tallow (%)	100	100	100

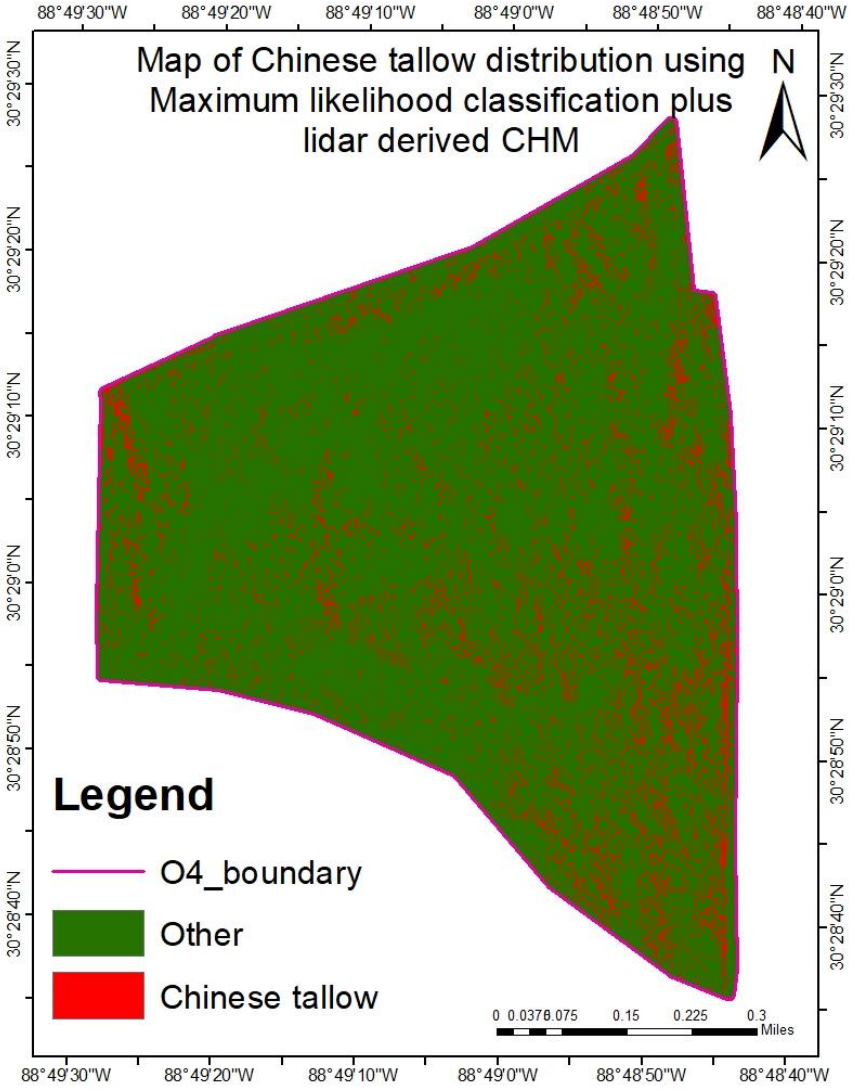

Figure 7. Map of O4 burn unit of Mississippi Sandhill Crane National Wildlife Refuge showing the distribution of Chinese tallow. The green area represents other (bare ground and other vegetation such as hardwood and pine) and red area represents the distribution of Chinese tallow. The figure shows distribution map of Chinese tallow using Maximum Likelihood classifier on NAIP imagery and CHM. This mapping approach has highest overall accuracy for classifying Chinese tallow among the classification approaches used.

The same method and dataset that produced highest overall accuracy and kappa coefficient gave good producer's accuracies and user's accuracies for classifying Chinese tallow on O4 burn unit of Mississippi Sandhill Crane National Wildlife Refuge. The producer's accuracy for Chinese tallow was 94.61% (Table 15) and the user's accuracy was 100%. The confusion matrix shows that Chinese tallow had 167 ground truth pixels, 158 out of those were correctly classified as Chinese tallow (Table 14). Hence, the producer's accuracy is 158/167=94.61%, which means 94.61% of time Chinese tallow was labelled as Chinese tallow on the classified image. Chinese tallow had a total of 158 classified pixels, all those classified pixels were classified correctly as Chinese tallow (Table 14). Hence, the user's accuracy is 158/158= 100%, which means that 100% of the area in classified image labelled as Chinese tallow (classified as Chinese tallow) was Chinese tallow on the ground.

Table 14. Confusion matrix obtained for maximum likelihood classifier using NAIP imagery and CHM for O4 burn unit of Mississippi Sandhill Crane National Wildlife Refuge (in pixels).

Ground Truth (Pixels)			
Class	Other	Chinese tallow	Total
Other classified	100	9	109
Chinese tallow classified	0	158	158
Total	100	167	267

Table 15. Confusion matrix obtained for maximum likelihood classifier using NAIP imagery and CHM for O4 burn unit of Mississippi Sandhill Crane National Wildlife Refuge (in percent).

Ground Truth (Percent)			
Class	Other	Chinese tallow	Total
Other classified	100	5.39	40.82
Chinese tallow classified	0	94.61	59.18
Total	100	100	100

2.4. Discussion

The study investigated techniques for mapping the distribution of Chinese tallow and Chinese privet within ecologically sensitive coastal areas, with focus on the coastal region of Alabama in the southeastern US. A combination of bands from NAIP imagery, CHM and CDM derived from lidar were examined for each classification approach. The overall accuracies, producer's accuracy, user's accuracy, and the agreement between known and predicted values (kappa coefficient) obtained from different classification approaches varied over the study area.

Among all classification approaches carried out on Mobile Tensaw Wildlife Management Area, RF produced good overall accuracy as compared to ISODATA clustering and Maximum Likelihood classifier. Jensen et al. (2020) and Shoot et al. (2021) have demonstrated the machine learning algorithm (e.g., RF) as a robust classifier for natural resource data. These findings are supported by Shoot et al. (2021), that showed the highest overall accuracy of 78% and a kappa of 0.66 obtained with the RF classification algorithm using hyperspectral vegetation indices and lidar-derived canopy height metrics. In general, RF outperformed ISODATA clustering and Maximum Likelihood classifier regarding overall classification accuracies. The classification accuracies for Chinese tallow were better with RF using lidar-derived variables integrated with NAIP imagery on Bon Secour area. Chan et al. (2012) supports that RF classifier achieves better classification results when multi-dimensional and multi-source data are used. Overall, improved classification results could be expected using RF in terms of overall accuracies.

On Mobile Tensaw Wildlife Management Area, the use of NAIP imagery only on RF produced good overall accuracy, however it was not able to detect and accurately classify Chinese privet in the study site (Figure 3). It is because Chinese privet is a shrub species, concealed under the canopy of Chinese tallow and other vegetation which makes the detection difficult. The same classification approach and dataset did not produce good accuracies for mapping Chinese tallow as well. It may be due to confusion of pixels of Chinese tallow with other classes. Among the classification approaches used with the same dataset, maximum likelihood classifier produced highest producer's accuracy for mapping Chinese tallow. Additionally, ISODATA classification produced highest user's accuracy for mapping Chinese tallow.

Since Chinese privet was not detected with RF using NAIP imagery only, we added CHM and CDM with a height cut-off of 7 m, prepared especially for Chinese privet to the

dataset. The maximum height recorded for Chinese privet in the study site was 7m therefore, the height cut-off of 7 m was selected. This classification approach and dataset that produced high overall accuracy and kappa coefficient did not produce highest accuracies for mapping Chinese privet however, this method helped to classify Chinese privet among RF used (Figure 4). It is suggested that for mapping invasive species concealed under canopy, models developed with specific height cutoffs favoring the height of species aids in detection of the species. Among the classification approaches used, maximum likelihood classifier used with NAIP, and CHM produced highest producer's accuracies for mapping Chinese privet. Additionally, maximum likelihood classifier used with NAIP, CHM and CDM used with height cutoff of 7m produced highest user's accuracies for mapping Chinese privet. We believe the highest overall accuracy might have been achieved, in this case with RF using a combined dataset of NAIP, CHM and CDM due to good classification accuracy of other classes (water, built up, coastal sand and other vegetation).

Among all classification approaches carried out on Bon Secour National Wildlife Refuge and o4 unit of Mississippi Sandhill Crane National Wildlife Refuge, Maximum Likelihood classifier using the CHM integrated with NAIP imagery produced better overall accuracy. The overall accuracy and PA for classifying Chinese tallow increased after adding the CHM to NAIP imagery. The addition of the CHM to NAIP imagery provided more information that improved the classification results. Specifically, the coastal sand class was separable from built-up areas, and grassland was more separable from Chinese tallow due to the addition of structural information from lidar. An increased overall accuracy was observed as a result. In general, the Maximum Likelihood classifier performed well over the smaller study site (Bon Secour National Wildlife Refuge) as compared to the larger study site (Mobile Tensaw Wildlife Management Area). Poala et al. (1995) demonstrated that the Maximum Likelihood classifier is sensitive to spectral properties of classes and performs poorly for larger area having heterogenous stands. Bon Secour area consists of homogeneous forest stands based on the field inventory. The area is dominated by forests, with a low portion of the area covered by water, built-up, grassland, and coastal sand. The separation of classes is straightforward, and there is less confusion between classes in the Bon Secour area. Similar is the case for O4 unit of Mississippi Sandhill Crane National Wildlife Refuge, the area is smaller and there is less confusion among classes. That is why smaller and homogeneous area was associated with better accuracy. For larger study areas,

acquiring NAIP imagery having phenological differences between the species and adding ancillary data such as texture, slope, and elevation that differentiates the species given their similar spectral properties may be helpful.

Adding lidar-derived variables to NAIP imagery increased the overall accuracy and kappa coefficient of the classification map compared to the overall accuracy and kappa coefficient obtained using NAIP imagery alone, regardless of the algorithm used. Since both study sites was within a coastal region, there are waterlogged areas. Grassland, shrubs, and algal concentration found in waterlogged areas were confused with trees using NAIP imagery alone, but the classes were more easily separated after adding lidar-derived variables. With the added CHM and CDM to the NAIP, vegetation structural information was added, which allowed for the separation of trees, from shrubs and grassland. Adding lidar to the NAIP imagery adds up as a bolster for Chinese tallow and Chinese privet classification. Studies have demonstrated the benefits of combining structural (lidar) and spectral (imagery) data for classification. Hantson et al. (2012) showed increased overall classification accuracy from 39% to 50% of the classifier using vegetation height from lidar. Kim et al. (2020) conveyed higher classification accuracy with the aerial imagery combined with lidar than to aerial imagery alone.

Most of the coastal region of southern Alabama are not accessible due to floodplains. This highlights the use of remote sensing techniques for potential mapping of invasives, especially on the inaccessible study sites. We suggest the use of drone survey for collecting presence and absence data of invasive species from the inaccessible areas for better accuracy. Species can be detected remotely, given distinct morphology, and seasonality. Cavender-Bares et al. (2020) showed that when the target invasive species has unique phenology, it is easier to distinguish invasives from native species (Cavender-Bares et al., 2020). For instance, Ill et al. (2002) showed that the leaves of Chinese tallow turn red during the fall season, when it is senescing, making it distinct from other native species. However, since freely available data (aerial NAIP imagery and airborne lidar) was used for the study, the data for the desired season, i.e., fall season, was not available. It is recommended to use the remotely sensed data of senescing season to avoid confusion between spectrally similar vegetation and Chinese tallow to attain better accuracy.

Joshi et al. (2004) conveyed that remote sensing has been most applied for mapping canopy-dominant species. Remote sensing techniques used for detecting invasive species have

mainly dealt with overstory invasive species. But all invasive species do not dominate the canopy. Many invasive plants of concern are understory species, where the application of remote sensing technique is tricky for species detection. Due to the difficulty of mapping understory invasive species, these invaders have received little attention. The detection of Chinese privet was difficult compared to the detection of Chinese tallow. It is a shrub species usually found mixed with other shrubs and tree species. In some wet areas, Chinese tallow and Chinese privet grew side by side. The classification of Chinese privet was not easy due to the difficulty in detecting Chinese privet as an understory shrub, concealed by the canopy. It was challenging to discern Chinese privet remotely and attain better accuracy for classifying them. A study conducted by Cash et a. (2020) levergaed the potential to map Chinese privet over a small area of 23 km^2 using freely available satellite imageries from Landsat 8 and Sentinel 2. Likewise, freely available remote sensing data such as NAIP imagery and the use of lidar-derived CDM with height cut off (7 m) was found to improve the accuracy of mapping Chinese privet over large spatial extent of 751 km^2.

2.5. Conclusion

The study examined different mapping approaches by utilizing free and publicly available remote sensing data for invasive species mapping. In Mobile Tensaw Wildlife Management Area, RF algorithm achieved the highest overall accuracy of 98.62% and a kappa coefficient of 0.86 using the CHM and CDM integrated with NAIP. In Bon Secour National Wildlife Refuge, the Maximum Likelihood classifier achieved the highest overall accuracy of 98.7% and a kappa coefficient of 0.97 using the CHM integrated with NAIP imagery. Regardless of the algorithms used, adding lidar-derived variables to NAIP imagery increased the overall accuracy of the classified map. The RF algorithm used with the addition of lidar-derived variables and NAIP imagery outperformed ISODATA and Maximum Likelihood classifier while classifying Chinese tallow and Chinese privet. For classifying Chinese tallow, the RF algorithm achieved the maximum PA and UA and a good kappa coefficient of 0.90 on the Bon Secour area using the CDM and CHM integrated with NAIP imagery. Using similar input data and classification algorithms, good PA and UA were obtained to classify Chinese privet on the Mobile Tensaw area.

The workflow used by this study offers an inexpensive, reliable, and high-resolution data framework alternative to purchasing commercial data. The study provides a spatially explicit baseline inventory map of vital invasive species of the region that contributes to developing a framework for broader-scale mapping.

References

Abdel-Rahman, E. M., Mutanga, O., Adam, E., & Ismail, R. (2014). Detecting Sirex noctilio grey-attacked and lightning-struck pine trees using airborne hyperspectral data, random forest and support vector machines classifiers. *ISPRS Journal of Photogrammetry, 88*, 48-59.

Ahmad, A., & Quegan, S. (2013). Comparative analysis of supervised and unsupervised classification on multispectral data. *Applied Mathematical Sciences, 7*(74), 3681-3694.

ALIPC. (2019). Alabama's 10 worst Invasive Weeds. https://www.se-eppc.org/alabama/

Asner, G. P., Knapp, D.E., Kennedy-Bowdoin, Ty., Jones, M.O., Martin, R. E., Boardman, J., and Hughes, R. F. (2008). Invasive species detection in Hawaiian rainforests using airborne imaging spectroscopy and Lidar. *Remote Sensing of Environment, 112*(5), 1942-1955.

Barnett, J. M. (2016). *The impact of Chinese privet (Ligustrum sinense) on the survival and re-establishment of native plants at the dallas floodway extension.* University of North Texas,

Benez-Secanho, F. J., Grebner, D. L., Ezell, A. W., & Grala, R. K. (2018). Financial trade-offs associated with controlling Chinese privet (*Ligustrum sinense* Lour.) in forestlands in the southern USA. *Journal of Forestry, 116*(3), 236-244.

Bork, E. W., & Su, J. G. (2007). Integrating LIDAR data and multispectral imagery for enhanced classification of rangeland vegetation: A meta analysis. *Remote Sensing of Environment, 111*(1), 11-24.

Bradley, B. A. J. B. i. (2014). Remote detection of invasive plants: a review of spectral, textural and phenological approaches. *16*(7), 1411-1425.

Breiman, L. (2001). Random forests. *Machine Learning, 45*(1), 5-32.

Bush, B. M., Ulyshen, M. D., & Batzer, D. P. (2020). Effects of Chinese privet (*Ligustrum sinense*) invasion on decomposition and litter-dwelling invertebrates in Southeastern US floodplain forests. *Biological Invasions, 22*(6), 1957-1965.

Cash, J. S., Anderson, C. J., & Marzen, L. (2020). Evaluating free and simple remote sensing methods for mapping Chinese privet (*Ligustrum sinense*) invasions in hardwood forests. *SN Applied Sciences, 2*(5), 1-11.

Cavender-Bares, J., Gamon, J. A., & Townsend, P. A. (2020). *Remote sensing of plant biodiversity*: Springer Nature.

Chan, J. C.-W., Beckers, P., Spanhove, T., & Borre, J. V. (2012). An evaluation of ensemble classifiers for mapping Natura 2000 heathland in Belgium using spaceborne angular hyperspectral (CHRIS/Proba) imagery. *International Journal of Applied Earth Observation and Geoinformation, 18*, 13-22.

Chuvieco, E. (2016). *Fundamentals of satellite remote sensing: An environmental approach*: CRC press.

Congalton, R. G., & Green, K. (2019). *Assessing the accuracy of remotely sensed data: principles and practices*: CRC press.

Dubayah, R. O., & Drake, J. B. (2000). Lidar remote sensing for forestry. *Journal of forestry, 98*(6), 44-46.

Ehrenfeld, J. G. (2010). Ecosystem consequences of biological invasions. *Annual review of ecology, evolution, systematics and biodiversity, 41*, 59-80.

Fantle-Lepczyk, J. E., Haubrock, P. J., Kramer, A. M., Cuthbert, R. N., Turbelin, A. J., Crystal-Ornelas, R., . . . Courchamp, F. (2022). Economic costs of biological invasions in the United States. *Science of the Total Environment, 806*, 151318.

Foard, M. (2014). *Causes and consequences of Chinese privet (Ligustrum sinense Lour.) invasion in hydrologically altered forested wetlands*: Arkansas State University.

Freeman, E., & Frescino, T. (2018). Modeling and Map Production using Random Forest and Related Stochastic Models.

Freeman, E., Frescino, T., & Moisen, G. (2009). ModelMap: An R package for modeling and map production using Random Forest and Stochastic Gradient Boosting. *USDA Forest Service, Rocky Mountain Research Station, 507*.

Gislason, P. O., Benediktsson, J. A., & Sveinsson, J. R. (2006). Random forests for land cover classification. *Pattern Recognition Letters, 27*(4), 294-300.

Ham, J., Chen, Y., Crawford, M. M., & Ghosh, J. (2005). Investigation of the random forest framework for classification of hyperspectral data. *IEEE Transactions on Geoscience and Remote Sensing, 43*(3), 492-501.

Hantson, W., Kooistra, L., & Slim, P. A. (2012). Mapping invasive woody species in coastal dunes in the N etherlands: a remote sensing approach using LIDAR and high-resolution aerial photographs. *Applied vegetation science, 15*(4), 536-547.

Hart, J. L., & Holmes, B. N. (2013). Relationships between *Ligustrum sinense* invasion, biodiversity, and development in a mixed bottomland forest. *Invasive Plant Science and Management, 6*(1), 175-186.

Hawthorne, T., Elmore, V., Strong, A., Bennett-Martin, P., Finnie, J., Parkman, J., . . . Reed, J. (2015). Mapping non-native invasive species and accessibility in an urban forest: A case study of participatory mapping and citizen science in Atlanta, Georgia. *Applied Geography, 56*, 187-198.

Hayes, M. M., Miller, S. N., & Murphy, M. A. (2014). High-resolution landcover classification using Random Forest. *Remote sensing letters, 5*(2), 112-121.

Heckbert, S., Costanza, R., Poloczanska, E., & Richardson, A. (2011). 12.10–Climate regulation as a service from estuarine and coastal ecosystems. *Treatise on estuarine and coastal science*, 199-216.

Hobbs, R., & Humphries, S. (1995). An Integrated Approach to the Ecology and Management of Plant Invasions. Conservational Biology, 9, 761-770. In.

Horning, N. (2010). *Random Forests: An algorithm for image classification and generation of continuous fields data sets.* Paper presented at the Proceedings of the International Conference on Geoinformatics for Spatial Infrastructure Development in Earth and Allied Sciences, Osaka, Japan.

Huang, C.-y., & Asner, G. P. (2009). Applications of remote sensing to alien invasive plant studies. *J Sensors, 9*(6), 4869-4889.

Ill, E. W. R., Nelson, G. A., Sapkota, S. K., Seeger, E. B., & Martella, K. D. (2002). Mapping Chinese tallow with color-infrared photography. *Photogrammetric Engineering, 68*(3), 251-255.

Isenburg, M. (2014). "LAStools - efficient LiDAR processing software" (version 141017, unlicensed).

Ismail, R., Mutanga, O., & Peerbhay, K. (2016). The identification and remote detection of alien invasive plants in commercial forests: An Overview. *South African Journal of Geomatics, 5*(1), 49-67.

Jensen, T., Seerup Hass, F., Seam Akbar, M., Holm Petersen, P., & Jokar Arsanjani, J. (2020). Employing machine learning for detection of invasive species using sentinel-2 and aviris data: The case of Kudzu in the United States. *Sustainability, 12*(9), 3544.

Joshi, C., De Leeuw, J., & Van Duren, I. C. (2004). *Remote sensing and GIS applications for mapping and spatial modelling of invasive species.* Paper presented at the Proceedings of ISPRS.

Kim, J., Popescu, S. C., Lopez, R. R., Wu, X. B., & Silvy, N. J. (2020). Vegetation mapping of No Name Key, Florida using lidar and multispectral remote sensing. *International Journal of Remote Sensing, 41*(24), 9469-9506.

Klepac, J., Rummer, R. B., Hanula, J. L., & Horn, S. (2007). Mechanical removal of Chinese privet. *Res. Pap. SRS-43. Asheville, NC: US Department of Agriculture, Forest Service, Southern Research Station. 5 p., 43*.

Liang, W., Abidi, M., Carrasco, L., McNelis, J., Tran, L., Li, Y., & Grant, J. (2020). Mapping vegetation at species level with high-resolution multispectral and lidar data over a large spatial area: a case study with Kudzu. *Remote Sensing, 12*(4), 609.

Loewenstein, N. J., & Loewenstein, E. (2005). Non-native plants in the understory of riparian forests across a land use gradient in the Southeast. *Urban Ecosystems, 8*(1), 79-91.

Matongera, T. N., Mutanga, O., Dube, T., & Lottering, R. T. (2018). Detection and mapping of bracken fern weeds using multispectral remotely sensed data: a review of progress and challenges. *Geocarto international, 33*(3), 209-224.

Michez, A., Piégay, H., Jonathan, L., Claessens, H., & Lejeune, P. (2016). Mapping of riparian invasive species with supervised classification of Unmanned Aerial System (UAS) imagery. *International Journal of Applied Earth Observation and Geoinformation, 44*, 88-94.

Miller, J. H., Lemke, D., Coulston, J., Wear, D. N., & Greis, J. G. (2013). The invasion of southern forests by nonnative plants: current and future occupation, with impacts, management strategies, and mitigation approaches. *178*, 397-456.

Montez, R. D., Saenz, D., Kley, M.-V., Van Kley, J., Nalian, A., & Farrish, K. (2021). The influence of Chinese tallow (*Triadica sebifera*) leaf litter on water quality and microbial community composition. *Aquatic Ecology, 55*(1), 265-282.

Ng, B., Quinete, N., Maldonado, S., Lugo, K., Purrinos, J., Briceño, H., & Gardinali, P. (2021). Understanding the occurrence and distribution of emerging pollutants and endocrine disruptors in sensitive coastal South Florida Ecosystems. *Science of the Total Environment, 757*, 143720.

Order, E. P. E. O. (1999). Invasive Species. *Fed. Regist., 64*, 6183–6186.

Popescu, S. C. (2007). Estimating biomass of individual pine trees using airborne lidar. *Biomass and Bioenergy, 31*(9), 646-655.

Ramsey, E., & Rangoonwala, A. (2018). Hyperspectral remote sensing of wetland vegetation. In *Advanced Applications in Remote Sensing of Agricultural Crops and Natural Vegetation* (pp. 219-245): CRC Press.

Randall, J. P. (2015). *Remote-Sensing Detection of Invasive Chinese Tallow (Triadica sebifera) in a Floodplain Environment.* Texas A&M University,

Sen, R., Goswami, S., & Chakraborty, B. (2019). *Jeffries-Matusita distance as a tool for feature selection.* Paper presented at the 2019 International Conference on Data Science and Engineering (ICDSE).

Shoot, C., Andersen, H.-E., Moskal, L. M., Babcock, C., Cook, B. D., & Morton, D. C. (2021). Classifying forest type in the national forest inventory context with airborne hyperspectral and lidar data. *Remote Sensing, 13*(10), 1863.

Survey, U. S. G. (2019a). Aerial imagery.

Survey, U. S. G. (2019b). United States Geological Survey 3D Elevation Program.
Ustin, S. L., DiPietro, D., Olmstead, K., Underwood, E., & Scheer, G. J. (2002). *Hyperspectral remote sensing for invasive species detection and mapping.* Paper presented at the IEEE International Geoscience and Remote Sensing Symposium.
Wang, H.-H. (2011). *Occupation, dispersal, and economic impact of major invasive plant species in southern US forests.* Texas A & M University,
Wilcove, D. S., Rothstein, D., Dubow, J., Phillips, A., & Losos, E. (1998). Quantifying threats to imperiled species in the United States. *BioScience, 48*(8), 607-615.
Wilcox, J., & Beck, C. W. (2007). Effects of *Ligustrum sinense* Lour.(Chinese privet) on abundance and diversity of songbirds and native plants in a southeastern nature preserve. *Southeastern Naturalist, 6*(3), 535-550.
Yang, S., Fan, Z., Liu, X., & Ezell, A. W. (2021). Predicting the spread of Chinese tallow (*Triadica sebifera*) in the southeastern United States forestland: Mechanism and risk factors at the regional scale. *Forest Ecology and Management, 482*, 118892.
Zedler, J. B., & Kercher, S. (2004). Causes and consequences of invasive plants in wetlands: opportunities, opportunists, and outcomes. *Critical Reviews in Plant Sciences, 23*(5), 431-452.
Zuberi, M. I., Gosaye, T., & Hossain, S. (2014). Potential threat of alien invasive species: Parthenium hysterophorus L. to subsistence agriculture in Ethiopia. *Sarhad Journal of Agriculture, 30*(1), 117-125.

Chapter 3: An assessment of the pattern and factors supporting spread of Chinese tallow in coastal plant community: A study conducted in Mississippi Sandhill Crane National Wildlife Refuge, Mississippi, USA.

3.1 Introduction

Southern forests from Virginia to Texas produce nearly 60% of the nation's timber products (Rauscher & Johnsen, 2004) and significantly contribute to the economy and ecosystem services in the United States (Sui, 2015). However, invasive plant species have threatened ecosystem functions, replaced native vegetation, and reduced forest productivity (Fan et al., 2018; Gan et al., 2009; Monty et al., 2013; Panetta & Gooden, 2017; Yang, 2019). *Triadica sebifera* (hereafter, Chinese tallow) is of concern because of its ability to replace the native vegetation and form a monotypic stands (Wang, 2011). Controlling the spread of Chinese tallow is of great concern as it is spreading rapidly from southern coastal areas to the inland.

Coastal forests of the southern United States are susceptible to the spread of invasive plant species following large-scale natural and anthropogenic disturbances such as hurricanes, wildland fires, and land-use changes (Barrow et al., 2005). Along the southern Gulf Coast, Chinese tallow was first introduced by the United States Department of Agriculture in southern Texas in the 1900s for use in the soap industry (Howes, 1949; Miller et al., 2013). It spread from southern Texas to coastal areas of Louisiana, Mississippi, and Alabama (Nepal et al., 2021). The invasion of Chinese tallow is a non-stationary process, with the spread varying across spatial and temporal scales and ecosystems, controlled by geographic/landscape characteristics and local site factors such as propagule pressure, life history of invading species, and recipient environment (Fan et al., 2021c).

Chinese tallow is a fast-growing, deciduous tree that can grow up to 60 feet (18.3 m) high and 3 feet (0.9 m) wide at maturity. Seeds are produced in large numbers and seed production can begin as early as three years of age (Renne et al., 2002). Due to the characteristics like more seed-producing capacity, good seed viability, easy seed dispersal modes, and ability to establish in a disturbed environment, Chinese tallow has sound spread and establishment rate. Seeds can germinate in a broad range of soil conditions, retain viability for at least five years, and are dispersed primarily by water and birds (Yang 2019). Fire, burial, water and bird dispersal

enhances seed germination rates. Furthermore, Chinese tallow is capable of root and stump sprouting following damage (Tian et al., 2017; Vanheuveln, 2016).

The stages of Chinese tallow invasion include seed dispersal, seed germination, seedling colonization, and sapling establishment (Fan et al., 2021b). After establishment, Chinese tallow starts to spread. Disturbances related to management activities (e.g., timber extraction, roadways, fire lines, and prescribed fire) and natural disturbances (e.g., flooding, hurricanes, stormwater, and wildfire) play a vital role in spread and establishment success (Fan et al., 2018). These intentional or unintentional disturbances create an ample niche opportunity for the spread and establishment of Chinese tallow. In addition, changes in environmental conditions (e.g., soil properties, soil moisture levels, and light penetration availability in the understory) often favor Chinese tallow growth post establishment (Tererai et al., 2015). High invasion severity is often observed along roadways, fire lines, ditches, trails, and within natural disturbances sites. Once established in these habitats, Chinese tallow may grow aggressively into surrounding areas, especially in areas with low competition, abundant light, and adjacency to water bodies.

Several studies have documented the impact of Chinese tallow on native forest ecosystems (Camarillo et al., 2015; Fan et al., 2021c; Montez et al., 2021; Saenz et al., 2013). Chinese tallow contains high tannins in the leaf litter, decomposing and leaching soluble nutrients faster than native species, which enhances its ability to alter the composition of microbial communities (Montez et al., 2021). Chinese tallow also has negative impacts on aquatic amphibian survival (Saenz et al., 2013), stand density of native tree species (Camarillo et al., 2015) and due to its aggressive growth, it has the potential to replace valuable bottomland forest (Nepal et al., 2021). Studies also show that the invasion of Chinese tallow has decreased the effectiveness of prescribed fires(Fan et al., 2021a), modifying the fire regime and functioning as a fire suppressor (Fan et al., 2021b).

If proper measures for controlling spread are not taken, the monotypic stands of Chinese tallow could completely replace the native vegetation in some situations (Camarillo et al., 2015; Tian et al., 2017; Yang, 2019; Yang et al., 2021). Elm/ash/cottonwood and oak/gum/cypress forests were vulnerable to Chinese tallow invasion compared to longleaf/slash pine forests (Nepal et al., 2021). However, Sui (2015) predicted that in next 60 years the highest Chinese tallow invasion would occur in longleaf/slash pine and oak/gum/cypress forests. Several direct and indirect interactive factors are involved in the spread and establishment of Chinese tallow.

The competitive interactions between Chinese tallow and native species are regulated by landscape features, characteristics of the recipient environment, and invasion stages of Chinese tallow within a specific ecosystem (Fan et al., 2018; Lockwood et al., 2013). In addition, disturbances such as hurricanes, tropical storms, timber extraction, prescribed fires, and construction of roads and fire lines also facilitate invasion (Fan et al., 2018; Yang et al., 2021). Factors supporting Chinese tallow spread are mainly birds, water movement, propagule pressure, distance to seed trees, tree density, canopy closure, elevation, and distance to the nearest road (Fan et al., 2021b; Fan et al., 2018; Fan et al., 2021c).

The objectives of this study were to understand the pattern of Chinese tallow spread and which community structures factors support Chinese tallow spread in the coastal region of the United States. Although past studies have reported the pattern of Chinese tallow spread and associated factors, generalization for decision-making is difficult without understanding every aspect of the community structure. The interactions at the community level and the complexities of Chinese tallow spread make it challenging to understand the actual facilitators of spread (Pile et al., 2017). The critical assessment of patterns and factors supporting the spread of Chinese tallow at the community level is limited. However, such an appraisal is urgently needed to aid the decision-making for proper management efforts to control the spread of Chinese tallow from the coastal region of the southeastern US to the islands.

3.2 Materials and Methods

A field inventory, consisting of measurements carried out at the community level within pine, hardwood, and Chinese tallow invaded communities, was executed in May 2021. The inventory was conducted in a 4.75 km^2 area within Mississippi Sandhill Crane National Wildlife Refuge where previous Chinese tallow studies have been conducted (Fan et al., 2021b). The collected field data was compiled and analyzed using correlation analysis and Zero Inflated Negative Binomial (ZINB) Regression analysis.

3.2.1 Study area

The study area is located within Mississippi Sandhill Crane National Wildlife Refuge (MSCNWR) in the coastal region of Mississippi (Figure 8). It is now a part of the Gulf Coast

National Wildlife Refuge Complex. The southern coastal region has a semi-tropical climate with an average annual temperature of 18 °C (64 °F). The temperature in the hottest month (July) and coldest month (January) averages 32 °C (90 °F) and 4°C (40°F), respectively. The region's average annual precipitation is 1,400 mm (56 inches) (Packard, 2012). The landforms consist of flat plains, marshes, river deltas, and wetlands. The study was carried out in an area of 4.75 km^2 within MSCNWR. The landscape is flat, waterlogged, and the soil is acidic. The primary community type found on the wildlife refuge area is wet pine savanna. However, within the area where the field inventory was carried out, shrubs, grasses and other herbaceous plants were present under pine and hardwoods.

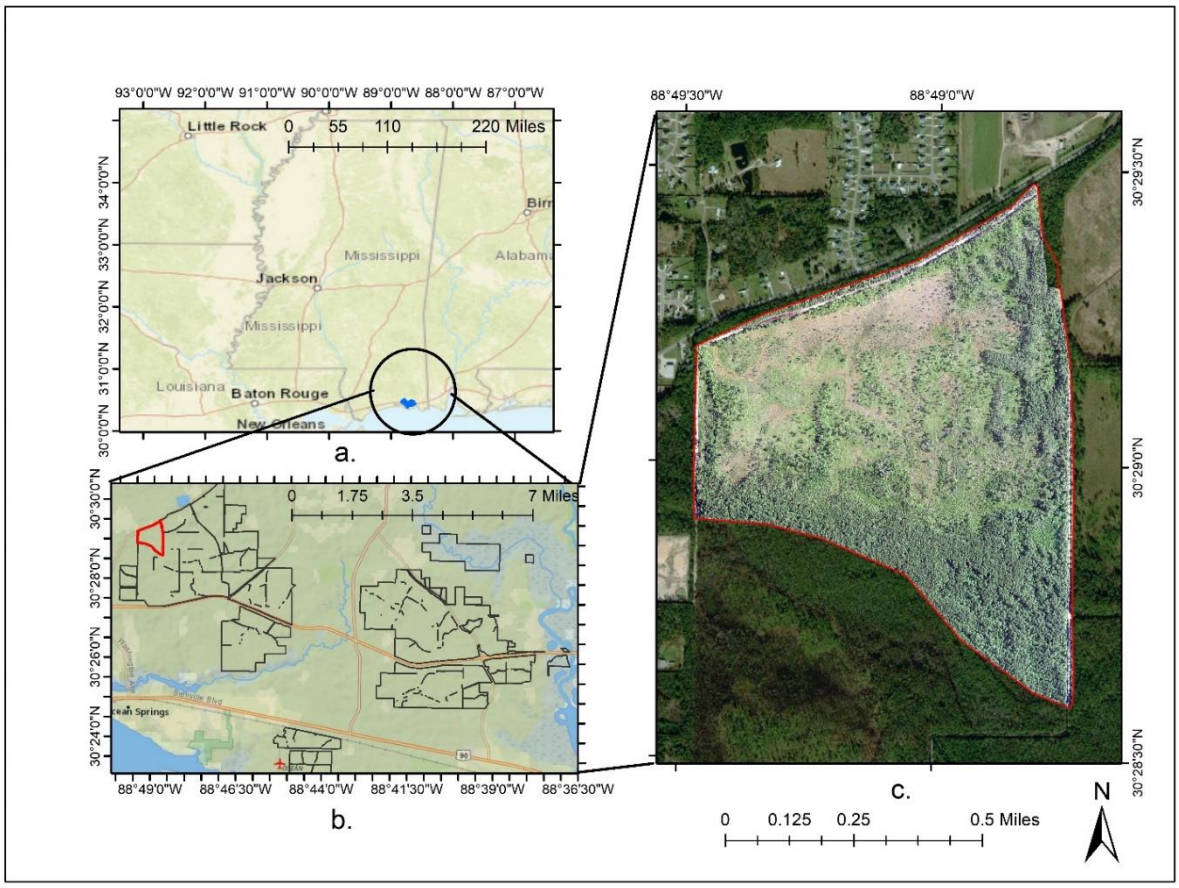

Figure 8. Map of the study area. a. Location of Mississippi Sandhill Crane National Wildlife Refuge in Mississippi state, b. Outline of east, west and south side blocks of MSCNWR, with O4 unit of west block highlighted in red, and c. O4 burn unit from MSCNWR (Section 3.2.2).

3.2.2 Data collection

To have a better understanding of the impact of different invasion degrees of Chinese tallow on growth of different vegetation types such as pine savanna, savanna, pine flatwoods, and hardwood forests, the study area, unit O4 of MSCNWR, was further classified into 21 stands

based on the overstory and understory coverage, structure, and compositions. Within each classified stand, Simple Random Sampling (SRS) method was applied. A total of 139 quadrats were recorded randomly within 21 patches and each of them had an area of 16 m^2. Quadrats were set up by using a field tape and the corners of each quadrat were established by using marking flags to create boundaries of each quadrat. Within each quadrat, field coordinates, soil moisture, Diameter at Breast Height (DBH), height, and number of overstory and midstory pine, hardwood were measured. Also, 5-year increments and 10-year increments of overstory and midstory pine trees were measured. Additionally, DBH, height, and number of mature trees and saplings of Chinese tallow were measured. Height and percentage cover of understory shrubs, grasses, Chinese tallow seedlings, and pine seedlings were also measured. Plot coordinates were recorded using GPS and soil moisture was measured using a soil moisture meter at the center of the plot (Moon City), at the depth of 4 inches. DBH was measured using diameter tape and heights were measured using a hypsometer. For the measurements of 5-year and 10-year increment of pine trees, an increment borer was used. Three midstory and three overstory trees were cored, if available on each quadrat. The heights of understory species were measured using a metallic measuring scale that has readings in inches or meters, where grid estimation (each quadrat has 16 grids) were used to predict coverage of understory vegetation.

The forest stands adjacent to roadways within the study unit had a higher degree of Chinese tallow invasion than the other stands in the unit. To better document the patchy Chinese tallow distribution within the study area, Line Transect Sampling (LTS) was carried out. LTS is a method to measure the abundance of plants in a centerline (Buckland et al., 2007). LTS was used to cover a large area of tallow dominant stands and 16 m^2 quadrats at every 5 m distance of the line transect were used to conduct field inventory in the distributed patches of Chinese tallow. A total of 80 tallow transect quadrats were recorded. The measurements similar to SRS method were carried out in quadrats measured using LTS method.

3.2.3 Data analysis

3.2.3.1 Correlation analysis

Correlation analysis was carried out to understand the relationship between Chinese tallow and other forest variables. Correlation analysis provides information on the linear relationship between two or more quantitative variables. Correlation coefficient values range

from -1 to +1. (Gogtay & Thatte, 2017). Correlation analysis was carried out to understand the significant relationship between Chinese tallow variables (such as density, height, basal area, and age of mature tree and saplings of Chinese tallow), Chinese tallow understory variables (such as percentage cover and height), and other variables such as moisture of each quadrat, density, height, basal area, 5-year increment, 10-year increment and age of pine overstory and midstory trees.

3.2.3.2 Inverse Distance Weighted (IDW) interpolation

To understand the pattern of Chinese tallow distribution, IDW interpolation was done using R software. IDW interpolation assumes that the rate of similarities between points is proportional to the inverse of distance between every point from their neighboring points (Setianto & Triandini, 2013). The main factor affecting the accuracy of inverse distance interpolation is the value of the power parameter p (Burrough & McDonnell, 1998).

Three different height classes of Chinese tallow on each quadrat were defined i.e., seedling, sapling and mature trees. These height classes were selected based on the previous studies conducted on the similar study site (Fan et al., 2018). Seedling included height class less than 1m, sapling covered height class from 1-3 m and mature trees included height above 3 m. The density of overstory, midstory Chinese tallow, and percentage cover of understory Chinese tallow seedlings was used as a response variable to model the IDW interpolation.

3.2.3.3 Zero inflated negative binomial (ZINB) regression analysis

The ZINB model was used at two levels. First, the model was applied to all 219 quadrats. Second, the model was used for 80 transect-level plots recorded specifically for Chinese tallow to understand the key factors associated with the distribution of size classes of Chinese tallow (e.g., mature trees, saplings, and seedlings). Generally, ZINB regression model is used to model count data that has an excess of zero counts, usually for over dispersed count variables. Since the density of mature trees, saplings and seedlings of Chinese tallow had excess zero (Figure 9), over dispersion and the variance was much greater than the mean, ZINB regression modeling was used. We followed a methodology that was developed in a previous study at a similar site (Fan et al., 2018). The pscl package from R software was used to run the model. The ZINB model combines two equations i.e., Count model and logit model to evaluate the impact of involved factors (predictors) on Chinese tallow density (response). The count model accounts for true 0

values and predicts count for those values which are not excess 0. On the other hand, the logit model accounts for excess 0 values (Moghimbeigi et al., 2008).

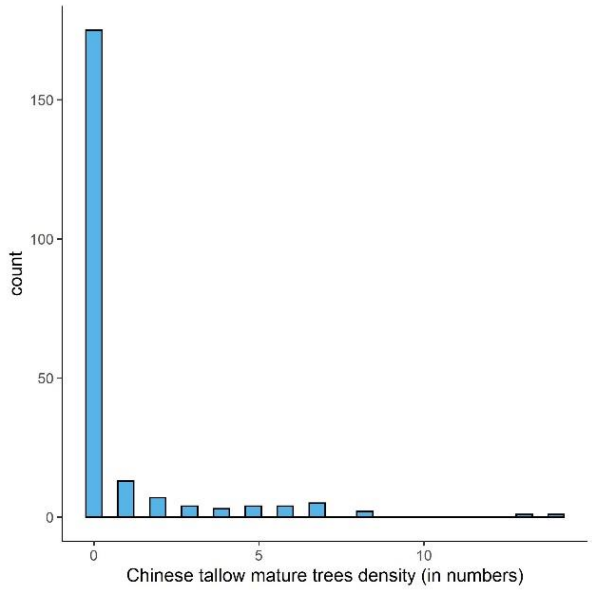

a.

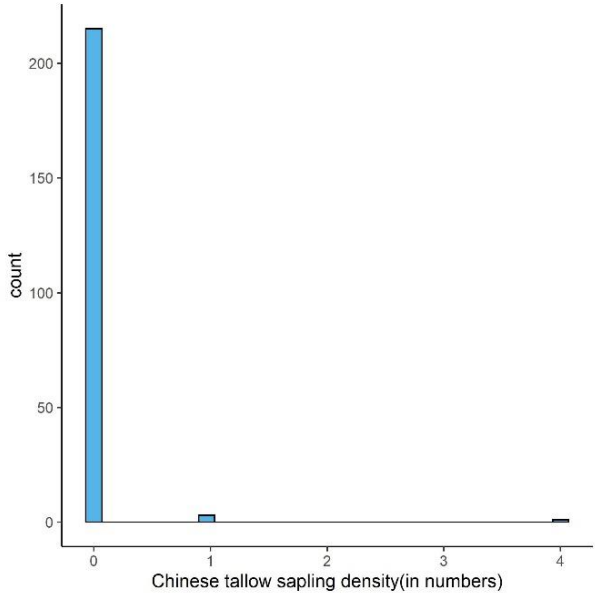

b.

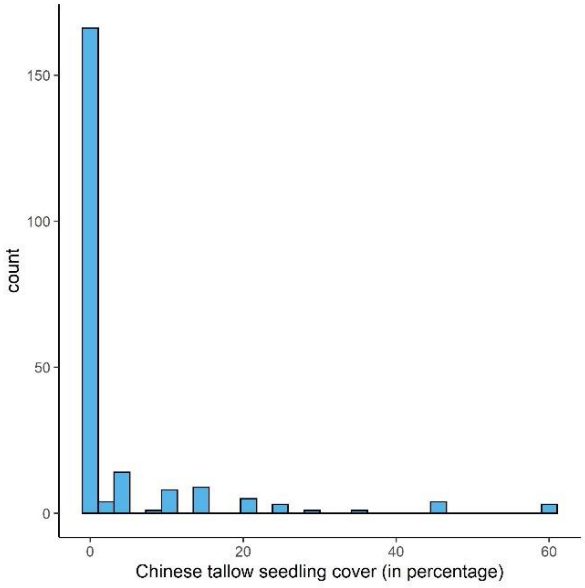

c.

Figure 9. Histograms showing zero inflation and over dispersion of 0 in count of Chinese tallow mature trees, saplings, and seedlings. a. Excess 0 in number of Chinese tallow mature tree density across Chinese tallow transect quadrats. b. Excess 0 in number of Chinese tallow sapling density. c. Excess 0 in percentage cover of Chinese tallow seedling.

3.3 Results

Results are summarized into three sub-sections. First, correlation analysis was performed to understand the relationship between Chinese tallow abundance and variables associated with pine, hardwood species, shrubs, and herbaceous grass cover. Second, IDW interpolation was carried out to understand the pattern of Chinese tallow spread in the study area. The interpolation was executed at three levels (mature trees, saplings, and seedlings of Chinese tallow) to understand the associated factors facilitating Chinese tallow seed dispersal and recruitment. Second, ZINB regression models were used for understanding contributing factors for seed dispersal, seedling establishment and growth of mature Chinese tallow trees. ZINB regression models were implemented using two datasets. First, using information of all 219 plots collected using SRS and second, using information of only 80 Chinese tallow plots recorded using LTS, to understand the factors associated with Chinese tallow seedling distribution, sapling establishment and density of mature trees.

3.3.1 Correlation analysis

Correlation analysis was performed in R software to understand the relationship between soil moisture, community structure (overstory, midstory and understory of pine and hardwood species) and abundance of Chinese tallow community structure (mature trees, saplings, and seedlings of Chinese tallow). Several studies have assessed the effects of topographic factors, vegetation type and plant community structure on Chinese tallow abundance (Battaglia et al., 2009; Bruce et al., 1995; Nepal et al., 2021). Chinese tallow was positively associated with overstory woody species and abundance in marsh sites (Battaglia et al., 2009). A study found longleaf/slash pine supported the abundance of Chinese tallow (Nepal et al., 2021). The abundance of Chinese tallow seedlings was also supported by Morella sp. (Battaglia et al., 2009).

We found a positive correlation between soil moisture and overall Chinese tallow density and basal area ($p < 0.05$) (Table 16). A positive correlation was also found between soil moisture and Chinese tallow seedling cover. This suggests that mature trees, and seedlings of Chinese tallow are found mostly in the areas with high moisture content within a range of 7-9 (out of 10). As expected, a significant positive relationship was also found between Chinese tallow mature density and understory Chinese tallow cover (Table 16). This supports our understanding that the

understory Chinese tallow are supported by the seed source obtained from the mature/overstory Chinese tallow trees.

Table 16. Table showing correlation between associated variables.

Variables	Correlation coefficient	p-value
Chinese tallow overall density and moisture	0.32	$p < 0.05$
Chinese tallow mature density and moisture	0.50	$p < 0.001$
Chinese tallow mature basal area and moisture	0.49	$p < 0.001$
Chinese tallow seedling cover and moisture	0.33	$p < 0.001$
Chinese tallow seedling cover and grass cover	-0.08	0.24
Chinese tallow sapling density and shrub cover	-0.13	0.06
Chinese tallow mature density and understory Chinese tallow cover	0.15	$p < 0.05$
Chinese tallow mature density and pine overstory density	-0.03	0.75
Chinese tallow mature density and pine midstory density	-0.08	0.52
Chinese tallow mature density and hardwood overstory density	-0.50	0.60
Chinese tallow mature density and hardwood midstory density	0.08	0.68

3.3.2 Pattern of Distribution of Chinese tallow using IDW interpolation

The study area is surrounded by roads on the eastern side and northern side of the study area (Figure 10a.). The northern roadside is close to a residential community whereas the eastern roadside lies within the wildlife refuge. The northern side of the study area has comparatively higher elevation, more water drainage with lower soil moisture content ranging around 1-6. The southern region of the study area had standing water, had low elevation (1.5-6m above mean sea level) (Teaford et al., 1995), and greater soil moisture content ranging around 4-9. The forest stands in the study area are not homogenous. The overstory within the southern portion is dominated by pine and hardwood trees which are favored by birds, (Hamel, 1992), and the overstory within the northern portion is dominated by pine trees. Based on field observation, the water flow obtained after rainfall, flowing from higher elevations of the northern region to lower

elevations of the southern region is prone to carry Chinese tallow seeds to the southern region of the study area.

With IDW interpolation, a clustered pattern of mature Chinese tallow was observed near the road that lies within the wildlife refuge and has abundant soil moisture. A small cluster of mature Chinese tallow was also observed adjacent to the northern road close to the residential community (Figure 10b). A dispersed pattern of Chinese tallow saplings (Figure 10c) and scattered Chinese tallow seedlings were also found near the eastern road within the wildlife refuge (Figure 10d). Some Chinese tallow seedlings were also found near the residential community.

Figure 10 provides the distribution of Chinese tallow size-classes (seedling, sapling and mature tree) based on field collected density information of Chinese tallow sapling, mature tree and percentage cover information of Chinese tallow seedling. Whereas Figure 7 presented in Chapter 2 gives distribution map of Chinese tallow with highest overall accuracy for classifying Chinese tallow obtained using maximum likelihood classifier on NAIP imagery and CHM among the classification algorithms used. Both figures produced show high abundance of Chinese tallow along the roadside within the national wildlife refuge.

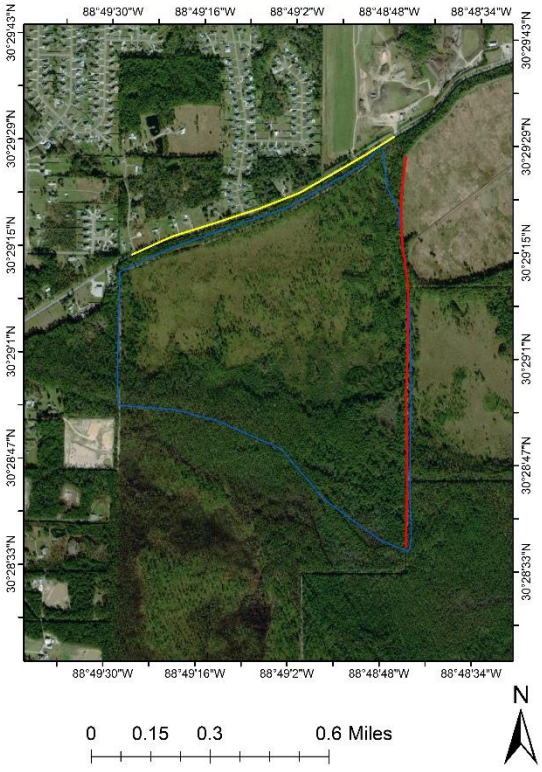

a. Aerial imagery of the study area.

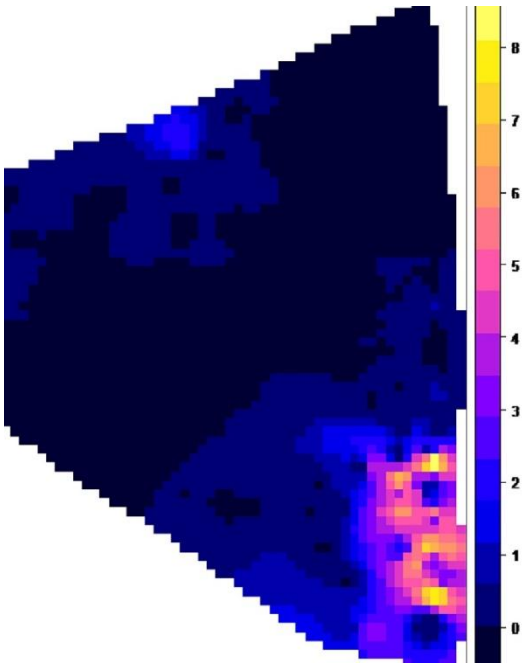

b. Pattern of mature Chinese tallow distribution.

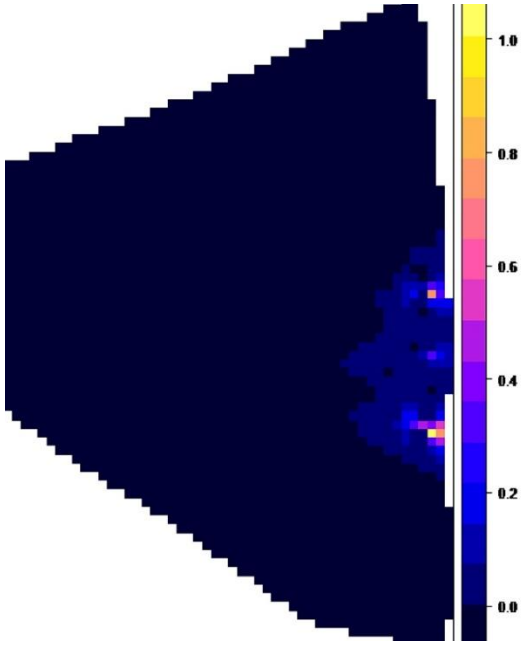

c. Chinese tallow sapling distribution.

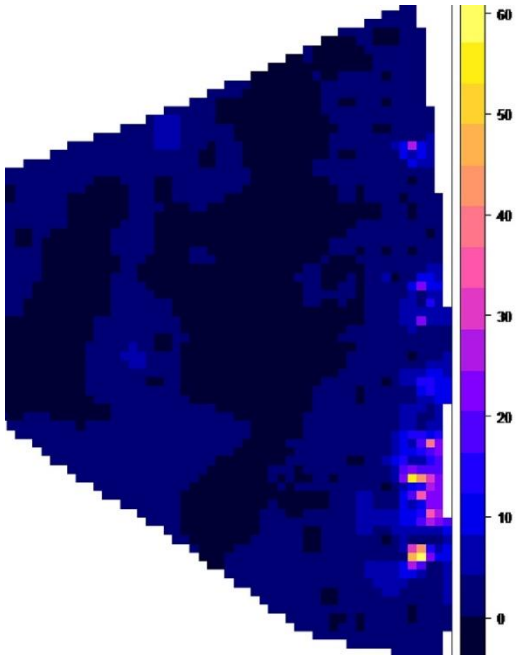

d. Chinese tallow seedling distribution.

Figure 10. Distribution of Chinese tallow in O4 unit of MSCNWR based on IDW interpolation.

The response variable used for overstory and midstory distribution of Chinese tallow was Chinese tallow density and the response variable used for understory Chinese tallow distribution was percentage cover of understory Chinese tallow. a. Aerial imagery of the study area where blue boundary represents outline of the study area, red line on the eastern side represents road within the wildlife reserve and yellow line on the northern side represents road close to residential community. b. Pattern of mature Chinese tallow distribution in the study area. The dark blue color shows no Chinese tallow density and yellow color shows highest Chinese tallow density. c. Pattern of Chinese tallow sapling distribution in the study area. d. Pattern of Chinese tallow seedling distribution in the study area.

3.3.3 Factors supporting spread of Chinese tallow at community level

ZINB regression models were used for understanding factors that support seed dispersal and Chinese tallow establishment (presence of mature trees). ZINB model conducted using all plot information showed no relationship between Chinese tallow tree and average pine overstory size, pine overstory 10-year growth and pine overstory age. Additionally, there was no relationship between mature Chinese tallow and average hardwood size (Table 17).

Table 17. Results of Zero Inflated Negative Binomial regression models using all plots.

Density of mature Chinese tallow and pine over story variables				
Count model coefficients (negative binomial with log link)				
	Estimate	Std. Error	z value	Pr(>|z|)
(Intercept)	-1.226	1.711	-0.717	0.474
Average Pine overstory size (ft^2/plot)	0.586	0.927	0.633	0.527
Pine over story 10-year growth (in)	0.066	0.722	0.091	0.927
Pine overstory age (number)	0.030	0.022	1.352	0.176
Log(theta)	1.716	1.499	1.145	0.252
Zero-inflation model coefficients (binomial with logit link):				
	Estimate	Std. Error	z value	Pr(>|z|)

(Intercept)	9.709	3.903	2.487	$p < 0.05$
Mature tallow and hardwood species				
Count model coefficients (negative binomial with log link:)				
	Estimate	Std. Error	z value	Pr(>|z|)
(Intercept)	1.306	0.626	2.085	$p < 0.05$
Hardwood size (ft^2/plot)	-10.971	13.787	-0.796	0.426
Log(theta)	0.427	1.457	0.293	0.769
Zero-inflation model coefficients (binomial with logit link):				
	Estimate	Std. Error	z value	Pr(>|z|)
(Intercept)	-0.796	1.289	-0.618	0.536

However, the ZINB model conducted using only tallow plots showed a positive relationship between mature Chinese tallow density, average pine overstory size and pine overstory age ($p < 0.05$) For each 1 ft^2/plot increase in pine overstory size, we found that mature Chinese tallow was 2.216 times as likely to be present ($p<0.05$). For each 1-year increase in pine overstory age, we found that mature Chinese tallow was 0.145 times as likely to be present ($p<0.005$) (Table 18). Since all mature Chinese tallow had age greater than 10 years, the 10-year increment of pine overstory had no effect on mature Chinese tallow density, there was no relationship between pine overstory 10-year growth and mature Chinese tallow (Table 18).

Table 18. Table showing results of Zero Inflated Negative Binomial regression models using only tallow plots.

For tallow plots, mature tallow density and pine variables				
Count model coefficients (negative binomial with log link:)				
	Estimate	Std. Error	z value	Pr(>|z|)
(Intercept)	-6.214	2.577	-2.411	$p < 0.05$
Pine overstory size (ft^2/plot)	2.216	1.041	2.127	$p < 0.05$
Pine over story 10-year growth (in)	-2.821	1.525	-1.849	0.064
Pine overstory age (number)	0.145	0.055	2.607	$p < 0.05$
Zero-inflation model coefficients (binomial with logit link):				
	Estimate	Std. Error	z value	Pr(>|z|)
(Intercept)	-128.08	11101.09	-0.012	0.991

3.4 Discussion

Abundant mature Chinese tallow trees were observed in areas with high soil moisture, ranging from 7-9. This suggests that mature Chinese tallow on this site were found mostly in areas with high availability of water or area that favors seed movement. A study similar to this found positive correlation between soil moisture and Chinese tallow abundance (Burns & Miller, 2004). An observational study noted high flood tolerance in Chinese tallow seedling (Jones & Sharitz, 1990). This may be the reason for the successful establishment of Chinese tallow seedlings in areas with high soil moisture. The areas having mature Chinese tallow trees supported the abundance of Chinese tallow seedlings. The presence of seedlings may be due to seed sources from mature Chinese tallow trees. Fan et al. (2021a) found similar results in the nearby Grand Bay National Wildlife Refuge, Mississippi, with high Chinese tallow seed and seedling densities in sites that were nearest to mature seed trees.

The distribution of Chinese tallow determined using IDW interpolation revealed a clustered pattern in the southeastern region of the study area. This section is characterized by

high seed availability, low elevation, flooded area and near proximity to a road within wildlife refuge (Figure 10a.). A good seed source, seed dispersal modes through birds and water are likely the direct contributing factors for the spread of Chinese tallow. Chinese tallow distribution was influenced by seed dispersal, low temps, and soil moisture (Pile et al., 2017). These findings are also supported by Fan et al. (2021b) conducted at MSCNWR that highlights the importance of seed sources, propagule pressure, proximity to roads for facilitating the spread of Chinese tallow and Fan et al. (2018) conducted at Grand Bay National Wildlife Refuge that noted the avian seed dispersal and water dispersal as the supporting factors for the abundance of Chinese tallow in the coastal region of Mississippi.

Additionally, other supporting factors such as abundance of overstory trees for bird habitat and water current for seed dispersal (due to low elevation), provide evidence for the abundance of Chinese tallow distribution in southeastern region of the study area. Based on the field observations, the areas with overstory pine trees had abundance of mature trees and seedlings of Chinese tallow. A study conducted in southern region of US shows that birds generally favor overstory trees for their habitat (Hamel, 1992). The abundance of overstory trees implies good habitat for birds. In addition, we observed a significant positive relationship between average size of overstory pine trees and density of mature Chinese tallow using ZINB model. This implies that the overstory trees, favored by birds for their habitat, are facilitating the Chinese tallow seed dispersal. Fan et al. (2021a) conveyed that the large abundance of tallow seedlings and saplings are due to high overstory tree in the study sites that facilitates birds.

Furthermore, some of the Chinese tallow seedlings were found distributed on the northern region of the study area. Based on the in-situ observations, the northern roadside of the study area is bordered by residential communities with Chinese tallow growing on these private properties (Figure 10a). Chinese tallow is preferred in southern residential communities due to its aesthetically pleasing leaves during fall. It may be possible that the seed source of such a small patch of Chinese tallow distribution is from home gardens of nearby residential communities.

There were not any overstory hardwood species and very few midstory hardwood species in tallow-invaded plots as compared to the non-tallow invaded plots as observed during the field data collection. We did not find any relationship between hardwood species and Chinese tallow density. However, studies such as Tian et al. (2017) and Yang et al. (2021) conducted in coastal region of Mississippi proclaimed the probability of Chinese tallow to outcompete hardwood

species. Furthermore, Nepal et al. (2021) reported the vulnerability of hardwood forest to the Chinese tallow invasion. Yang et al. (2021) and Sui et al. (2015) added that it is easier for Chinese tallow to invade hardwood forests as compared to pine forests.

Fan et al. (2021a) demonstrated that biological invasion is regulated by community structure, and the obtained findings from the study provide evidence in support of this. The seed dispersal, establishment and distribution of Chinese tallow depends on different factors of plant community. We observed that direct and contributing factors along with community characteristics play a vital role in influencing the spread and pattern of Chinese tallow invasion.

3.5 Conclusion

The distribution of Chinese tallow in the study area revealed a clustered pattern with the concentrated density of Chinese tallow in southeastern region of the study area, characterized by good seed source, reliable modes of seed dispersal, and high soil moisture content. For the spread of Chinese tallow in the specific region of the study area, several supporting factors were found. The direct contributing factors for the spread of Chinese tallow were identified as good source of propagule pressure and seed dissemination routes i.e., through birds and water. Additional factors that helped the spread of Chinese tallow included the existence of high soil moisture, low elevation, proximity to road, abundance of overstory trees for bird habitat, and overland water flow for seed dissemination. Furthermore, Chinese tallow seed dissemination appeared to be aided by overstory pine trees, which birds like for their habitat. The study's findings demonstrate how community structure can affect Chinese tallow's distribution. We conclude that the distribution and pattern of the Chinese tallow invasion are significantly influenced by both direct and indirect supporting factors as well as community characteristics.

References

Barrow, W., Randall, L. J., Woodrey, M., Cox, J., Riley, C., Hamilton, R., & Eberly, C. (2005). *Coastal forests of the Gulf of Mexico: a description and some thoughts on their conservation.* Paper presented at the In: Ralph, C. John; Rich, Terrell D., editors 2005. Bird Conservation Implementation and Integration in the Americas: Proceedings of the Third International Partners in Flight Conference. 2002 March 20-24; Asilomar, California, Volume 1 Gen. Tech. Rep. PSW-GTR-191. Albany, CA: US Dept. of Agriculture, Forest Service, Pacific Southwest Research Station.

Battaglia, L. L., Denslow, J. S., Inczauskis, J. R., & Baer, S. G. (2009). Effects of native vegetation on invasion success of Chinese tallow in a floating marsh ecosystem. *Journal of Ecology, 97*(2), 239-246.

Bruce, K. A., Cameron, G. N., & Harcombe, P. A. (1995). Initiation of a new woodland type on the Texas coastal prairie by the Chinese tallow tree (Sapium sebiferum (L.) Roxb.). *Bulletin of the Torrey Botanical Club*, 215-225.

Buckland, S. T., Borchers, D. L., Johnston, A., Henrys, P. A., & Marques, T. A. (2007). Line transect methods for plant surveys. *Biometrics, 63*(4), 989-998.

Burns, J. H., & Miller, T. E. (2004). Invasion of Chinese tallow (*Sapium sebiferum*) in the Lake Jackson area, northern Florida. *The American midland naturalist, 152*(2), 410-417.

Burrough, P. A., & McDonnell, R. A. (1998). Creating continuous surfaces from point data. *Principles of Geographic Information Systems. Oxford University Press, Oxford, UK*.

Camarillo, S. A., Stovall, J. P., & Sunda, C. (2015). The impact of Chinese tallow (*Triadica sebifera*) on stand dynamics in bottomland hardwood forests. *Forest Ecology and Management, 344*, 10-19.

Fan, Z., Song, A., Dong, L., Alexander, H. D., Yang, S., Cheng, N., & Pitchford, J. L. (2021a). Fire effects on post-invasion spread of Chinese tallow (*Triadica sebifera*) in wet pine flatwood ecosystems in the southeastern United States. *Forest Ecology and Management, 500*, 119658.

Fan, Z., Yang, S., Cheng, N., Liu, X., Song, A., & Dong, L. (2021b). Invasibility of fire-managed ecosystems to the Chinese tallow tree (*Triadica sebifera*) in the lower Gulf Coastal Plain, USA: Mechanisms and key factors at the landscape level. *Forest Ecology and Management 479*, 118539.

Fan, Z., Yang, S., & Liu, X. (2018). Spatiotemporal patterns and mechanisms of Chinese tallowtree (*Triadica sebifera*) spread along edge habitat in a coastal landscape, Mississippi, USA. *Invasive Plant Science Management, 11*(3), 117-126.

Fan, Z., Yang, S., Loewenstein, N. J., Cheng, N., Nepal, S., Pitchford, J. L., . . . Stone, D. (2021c). Modeling spatial variations of the invasibility of slash pine flatwoods to Chinese tallow (*Triadica sebifera*) invasion: Mechanisms and key factors at the microscale. *Forest Ecology and Management, 482*, 118798.

Gan, J., Miller, J. H., Wang, H., & Taylor, J. W. (2009). Invasion of tallow tree into southern US forests: influencing factors and implications for mitigation. *Canadian journal of forest research, 39*(7), 1346-1356.

Gogtay, N. J., & Thatte, U. M. (2017). Principles of correlation analysis. *Journal of the Association of Physicians of India, 65*(3), 78-81.

Hamel, P. B. (1992). *Land manager's guide to the birds of the South* (Vol. 22). United States. Forest Service. Southern Region: Nature Conservancy.

Howes, F. (1949). The Chinese tallow tree (*Sapium sebiferum Roxb*.): a source of drying oil. *Kew Bulletin, 4*(4), 573-580.

Jones, R. H., & Sharitz, R. R. (1990). Effects of root competition and flooding on growth of Chinese tallow tree seedlings. *Canadian journal of forest research, 20*(5), 573-578.

Lockwood, J. L., Hoopes, M. F., & Marchetti, M. P. (2013). *Invasion ecology*: John Wiley & Sons.

Miller, J. H., Lemke, D., Coulston, J., Wear, D. N., & Greis, J. G. (2013). The invasion of southern forests by nonnative plants: current and future occupation, with impacts, management strategies, and mitigation approaches. *178*, 397-456.

Moghimbeigi, A., Eshraghian, M. R., Mohammad, K., & Mcardle, B. (2008). Multilevel zero-inflated negative binomial regression modeling for over-dispersed count data with extra zeros. *Journal of Applied Statistics, 35*(10), 1193-1202.

Montez, R. D., Saenz, D., Kley, M.-V., Van Kley, J., Nalian, A., & Farrish, K. (2021). The influence of Chinese tallow (*Triadica sebifera*) leaf litter on water quality and microbial community composition. *Aquatic Ecology, 55*(1), 265-282.

Monty, M. F., Florens, F. V., & Baider, C. (2013). Invasive alien plants elicit reduced production of flowers and fruits in various native forest species on the tropical island of Mauritius (Mascarenes, Indian Ocean). *Tropical Conservation Science, 6*(1), 35-49.

Nepal, S., Moser, W. K., & Fan, Z. (2021). Spatiotemporal Invasion Severity of Chinese Tallow (*Triadica sebifera*) and Invasibility of Forest Types in Southern US Forestlands. *Forest Science, 67*(5), 491-500.

Packard, V. L. (2012). Physicalgeography. net. *Reference Reviews*.

Panetta, F. D., & Gooden, B. (2017). Managing for biodiversity: impact and action thresholds for invasive plants in natural ecosystems.

Pile, L. S., Wang, G. G., Stovall, J. P., Siemann, E., Wheeler, G. S., & Gabler, C. A. (2017). Mechanisms of Chinese tallow (*Triadica sebifera*) invasion and their management implications–a review. *Forest Ecology and Management, 404*, 1-13.

Rauscher, H. M., & Johnsen, K. (2004). *Southern forest science: past, present, and future* (Vol. 75): Southern Research Station.

Renne, I. J., Barrow Jr, W. C., Johnson Randall, L. A., & Bridges Jr, W. C. (2002). Generalized avian dispersal syndrome contributes to Chinese tallow tree (*Sapium sebiferum, Euphorbiaceae*) invasiveness. *Diversity Distributions, 8*(5), 285-295.

Saenz, D., Fucik, E. M., & Kwiatkowski, M. A. (2013). Synergistic effects of the invasive Chinese tallow (*Triadica sebifera*) and climate change on aquatic amphibian survival. *Ecology and evolution, 3*(14), 4828-4840.

Setianto, A., & Triandini, T. (2013). Comparison of kriging and inverse distance weighted (IDW) interpolation methods in lineament extraction and analysis. *Journal of Applied Geology, 5*(1).

Sui, Z. (2015). *Modeling tree species distribution and dynamics under a changing climate, natural disturbances, and harvest alternatives in the southern United States*: Mississippi State University.

Teaford, J., Lewis, P., & Johnson, D. (1995). Mississippi Pine Savannahs, Pine Flatwoods, and Forested Bayheads: Wetland Delineation, Evaluation, and Mitigation Considerations. *JW Teaford Company, Vicksburg, Mississippi*, 53.

Tererai, F., Gaertner, M., Jacobs, S. M., & Richardson, D. M. (2015). Resilience of invaded riparian landscapes: the potential role of soil-stored seed banks. *Environmental Management, 55*(1), 86-99.

Tian, N., Fan, Z., Matney, T. G., & Schultz, E. B. (2017). Growth and stem profiles of invasive Triadica sebifera in the Mississippi coast of the United States. *Forest Science, 63*(6), 569-576.

Vanheuveln, H. (2016). *Chinese tallow tree (Triadica sebifera) management and seed biology.* University of Florida,

Wang, H.-H. (2011). *Occupation, dispersal, and economic impact of major invasive plant species in southern US forests.* Texas A & M University,

Yang, S. (2019). Distribution and spread mechanisms of Chinese tallow (*Triadica sebifera*) at multiple spatial scales within forests in the southeastern United States.

Yang, S., Fan, Z., Liu, X., & Ezell, A. W. (2021). Predicting the spread of Chinese tallow (*Triadica sebifera*) in the southeastern United States forestland: Mechanism and risk factors at the regional scale. *Forest Ecology and Management, 482*, 118892.

Chapter 4: Conclusion

Due to the limited research on using remote sensing data for detecting Chinese tallow and Chinese privet over a broad spatial extent, an exploratory study to investigate the potential of free and open access remote sensing data on detecting and mapping the distribution of crucial invasive species was conducted. The initial, spatially comprehensive baseline map of invasive species obtained from the study is expected to support larger-scale mapping. Compared to purchasing commercial data, the workflow employed in this study provides a low-cost, replicable, and reliable data framework. Specifically, the freely available high-resolution multi-spectral aerial imagery such as National Agriculture Imagery Program (NAIP) and airborne lidar data downloaded from United States Geological Survey 3D Elevation Program (USGS 3DEP) were used for the study. From the implementation and comparison of multiple image classification approaches, a maximum overall accuracy of 98.62% and kappa coefficient of 0.86 was achieved using Random Forest (RF) model with lidar-derived products and NAIP imagery. Regardless of the algorithms used, adding lidar-derived variables to NAIP imagery increased the overall accuracy of the classified map. Moreover, the RF algorithm used with addition of lidar-derived variables and NAIP imagery was found feasible to classify Chinese tallow and Chinese privet as compared to using NAIP imagery alone.

Studies show that airborne lidar has been used effectively to map invasive species, especially, tree species. However, due to limitations related to temporal resolutions of airborne sensors, it may not be as effective in mapping invasive species of interest. Additionally, the temporal resolution of NAIP imagery limits the information about species of interest for desired seasons. Additionally, if the species of interest is masked by overstory species, it is difficult to discern the species from imagery. In this study, we faced difficulty in detecting Chinese privet as an understory shrub, concealed under hardwood trees with similar spectral reflectance. Hence, we tried improving the accuracy of mapping the distribution of Chinese privet using lidar derived Canopy Height Model (CHM) and Canopy Density Model (CDM) integrated with NAIP imagery. With the RF algorithm, Chinese privet was not detected from NAIP imagery, NAIP imagery integrated with CHM and NAIP imagery integrated with CHM and CDM having the height cutoff of 40 m. After adding the CDM with a height cutoff of 7m, Chinese privet was detected. This suggests that for mapping invasive species concealed under canopy, models

developed with specific height cutoffs favoring the height of species aids in detection of the invasive species. In this case, the maximum height of Chinese privet recorded in the study site was 7m, hence developing CDM with a height cut-off of 7m was quite beneficial to detect Chinese privet in the study area.

If the species of interest is abundantly distributed over the study site, high resolution aerial images such as NAIP imagery, with 1m spatial resolution, are quite useful, but if the species of interest is sparsely distributed, then detection of target species may be difficult. Ramsey's studies hypothesized the feasibility to detect Chinese tallow during the fall months, when it is senescing with distinct red color (Ill et al., 2002; Ramsey & Rangoonwala, 2018). However, such a methodology that relies on spectral differences between vegetation is prone to create a confusion between other senescent vegetation and Chinese tallow, unless multitemporal datasets are leveraged. Additionally, not all the plants senesce at the same rate, hence it is difficult to identify Chinese tallow from NAIP imagery only. In this case, the CHM and CDM derived from lidar enhances the potential of multispectral NAIP imagery to detect Chinese tallow. There are also opportunities for investigating the use of other machine learning algorithms such as Support Vector Machine (SVM) and Stochastic Gradient Boosting, using integrated NAIP imagery and lidar data, for increasing the accuracy of Chinese tallow and Chinese privet detection. A study found higher accuracy for mapping invasive species using SVM as compared to RF and object-based classification. (Liang et al., 2020).

The second study, presented in Chapter 3, provides an understanding about the spread pattern and factors supporting the spread of Chinese tallow in MSCNWR. The knowledge about factors that contribute the spread of Chinese tallow aids in Chinese tallow management decisions in future. The distribution of Chinese tallow was observed in areas characterized by good seed source, reliable modes of seed dispersal, and soil moisture. Numerous contributing factors were discovered for the proliferation of Chinese tallow in the study area. Good sources of propagule pressure and seed dissemination pathways, such as through birds and water, were found to be the direct contributing factors for the spread of Chinese tallow. High soil moisture, elevation, light availability, proximity to road, forest types, abundance of overstory trees for bird habitat, and water current for seed dissemination were additional elements that contributed to the spread of Chinese tallow (Fan et al., 2018; Fan et al., 2021; Pile et al., 2017).

The results of the study show clustered pattern of Chinese tallow distribution, influence of community structure on germination, establishment, and growth of Chinese tallow. We concluded that both direct and indirect supporting factors, as well as community characteristics, have a major impact on the prevalence and pattern of the Chinese tallow invasion. Since the best time to control invasive plant is at the early stages of its spread, this study provides information on where dispersed Chinese tallow is likely to establish. The pattern and risk factors of Chinese tallow spread can be accounted as hot spots for prioritizing control measures.

For the management of Chinese tallow invasion in southern coastal areas of the US, direct and indirect supporting factors of Chinese tallow spread should be considered. For instance, to reduce Chinese tallow spread from edge to interior, all tallow seed trees should be removed along the edges of road. Areas prone to have accumulated water should be monitored regularly for the early detection of Chinese tallow. Management activities such as timber extraction, prescribed fire, constructing fire lines and roads should be evaluated carefully to reduce the risk of potential Chinese tallow invasion. Control measures such as prescribed burn, mechanical removal, or herbicide treatment should be conducted timely. It might be possible for complete removal of Chinese tallow from small target sites, but removal from large areas (across landscapes) may be challenging. Hence, it is still necessary to comprehend the driving forces behind invasion from an integrated, multitemporal, and multiscale perspective at the level of individual establishment, population expansion, and post-invasion dissemination at a landscape level. Additionally, if there are seed trees within residential communities, such as adjacent to the Mississippi Crane National Wildlife Refuge, efforts undertaken inside wildlife refuge for controlling Chinese tallow will likely be in vain. Therefore, if practical, it is highly recommended that the wildlife refuge conducts an awareness campaign to remove Chinese tallow seed tress from surrounding residential communities and disseminates information about the ecological and economic impacts of invasive plant species on native ecosystems.

References

Fan, Z., Yang, S., & Liu, X. (2018). Spatiotemporal patterns and mechanisms of Chinese tallowtree (*Triadica sebifera*) spread along edge habitat in a coastal landscape, Mississippi, USA. *Invasive Plant Science Management, 11*(3), 117-126.

Fan, Z., Yang, S., Loewenstein, N. J., Cheng, N., Nepal, S., Pitchford, J. L., . . . Stone, D. (2021). Modeling spatial variations of the invasibility of slash pine flatwoods to Chinese tallow (*Triadica sebifera*) invasion: Mechanisms and key factors at the microscale. *Forest Ecology and Management, 482*, 118798.

Ill, E. W. R., Nelson, G. A., Sapkota, S. K., Seeger, E. B., & Martella, K. D. (2002). Mapping Chinese tallow with color-infrared photography. *Photogrammetric Engineering, 68*(3), 251-255.

Liang, W., Abidi, M., Carrasco, L., McNelis, J., Tran, L., Li, Y., & Grant, J. (2020). Mapping vegetation at species level with high-resolution multispectral and lidar data over a large spatial area: a case study with Kudzu. *Remote Sensing, 12*(4), 609.

Pile, L. S., Wang, G. G., Stovall, J. P., Siemann, E., Wheeler, G. S., & Gabler, C. A. (2017). Mechanisms of Chinese tallow (*Triadica sebifera*) invasion and their management implications–a review. *Forest Ecology and Management, 404*, 1-13.

Ramsey, E., & Rangoonwala, A. (2018). Hyperspectral remote sensing of wetland vegetation. In *Advanced Applications in Remote Sensing of Agricultural Crops and Natural Vegetation* (pp. 219-245): CRC Press.